

Theranostics

2026; 16(2): 689-711. doi: 10.7150/thno.112163

Research Paper

CCL5 promotes angiotensin II-induced cardiac remodeling through regulation of platelet-driven M2 macrophage polarization

Silin Lv¹,², Mingxuan Zhou¹,², Tiegang Li¹,², Zifan Zeng¹,², Zheng Yan¹,², Yufang Hou¹,², Liu Yang¹,², Fang Zhang¹,², Wenyi Zhao¹,², Yixin Zhou¹,², Min Yang¹,² \boxtimes

- 1. State Key Laboratory of Bioactive Substance and Function of Natural Medicines, Institute of Materia Medica, Chinese Academy of Medical Sciences and Peking Union Medical College, Beijing 100050, China.
- 2. State Key Laboratory of Digestive Health, Institute of Materia Medica, Chinese Academy of Medical Sciences and Peking Union Medical College, Beijing 100050, China.

☑ Corresponding author: Min Yang, State Key Laboratory of Bioactive Substance and Function of Natural Medicines, State Key Laboratory of Digestive Health, Institute of Materia Medica, Chinese Academy of Medical Sciences and Peking Union Medical College, No. 2 Nanwei Road, Beijing 100050, China. E-mail: minyang@imm.ac.cn, Tel: +86(10)63015871, Fax: +86(10)63017757.

© The author(s). This is an open access article distributed under the terms of the Creative Commons Attribution License (https://creativecommons.org/licenses/by/4.0/). See https://ivyspring.com/terms for full terms and conditions.

Received: 2025.02.14; Accepted: 2025.09.26; Published: 2026.01.01

Abstract

Rationale: Sustained hypertension induces adverse cardiac remodeling. Platelet activation is instrumental in exacerbating inflammation by engaging with macrophages. C-C chemokine motif ligand 5 (CCL5) is contained within platelet α -granules, and released following platelet activation. This work delineated the specific contributions of CCL5 to platelet function, platelet-induced macrophage polarization, and hypertensive cardiac remodeling.

Methods: CCL5 knockout (KO) mice infused with Angiotensin II (Ang II) were used to identify the role of CCL5 *in vivo*. CCL5 absence on platelet activation were evaluated on washed platelets. Two distinct models of platelet depletion and reconstitution were utilized to investigate the impact of platelets lacking CCL5. An *in vitro* co-culture system was established to explore the roles of CCL5-mediated platelet activation in M2 macrophage polarization.

Results: CCL5 KO attenuated the adverse cardiac effects induced by Ang II, including fibrosis, hypertrophy, and functional impairment, accompanied by reduced platelet activation and M2 macrophage polarization in cardiac tissue. Platelet inhibitor administration and platelet depletion/reconstitution experiments revealed that the suppression of platelet activation by CCL5 KO contributed to the amelioration of Ang II-promoted cardiac M2 macrophage polarization and cardiac remodeling. CCL5 KO markedly suppressed the activation of TGF-β1 and NF-κB signaling, an effect observed both in cardiac tissue from Ang II-infused mice and in platelets following ADP stimulation *in vitro*. In *in vitro* co-culture systems, rmTGF-β1 reversed CCL5 KO platelet-impaired M2 macrophage polarization. NF-κB inhibition abolished recombinant CCL5 (rmCCL5)-induced platelet activation, while blocking antibodies against CCR1 and CCR3 inhibited rmCCL5-induced NF-κB signaling and platelet activation.

Conclusions: These findings underscore the detrimental role of CCL5-mediated platelet activation in promoting M2 macrophage polarization during hypertensive cardiac remodeling and elucidate the molecular mechanism that CCL5 facilitates platelet-derived TGF-β1 signaling by promoting NF-κB activation *via* CCR1 and CCR3 receptors. These findings support CCL5 inhibition as a promising strategy against inflammation and cardiac damage.

Keywords: CCL5, hypertension, cardiac remodeling, platelet inflammation, M2 macrophage

Introduction

Hypertension-induced adverse cardiac remodeling, characterized by left ventricular (LV) hypertrophy and fibrosis, is a major driver of progression toward heart failure [1]. Angiotensin II (Ang II) contributes significantly to the development

of hypertension and drives the process of cardiac remodeling [2]. Ang II triggers a series of cardiac inflammatory responses, including immune cell recruitment, pro-fibrotic M2 macrophage polarization, and upregulation of inflammatory

cytokines [3-5]. Research indicates that inhibiting key inflammatory mediators or modulating immunocytes can mitigate cardiac remodeling prompted by Ang II [4, 5]. Therefore, a deeper understanding of the underlying immuno-inflammatory pathways in hypertensive cardiac remodeling is essential for preventing and treating hypertensive cardiac injury and heart failure.

Accumulating evidence points to the essential involvement of platelets in inflammatory processes, including their interaction with, stimulation of, and regulation of T cells, neutrophils, monocytes, and macrophages [6]. Platelets contribute to hypertensive organ damage by modulating the inflammatory response [7]. In response to circulatory changes such as endothelial cell damage, vessel wall injury, or hemodynamic abnormalities, platelets undergo morphological changes and modulate inflammation secreting factors and interactions inflammatory cells [6]. Using experimental models of pressure overload, ventricular fibrosis is associated with platelet-derived TGF-β1 [8]. Pharmacological inhibition of platelets or genetic TGF-β1 depletion platelets markedly alleviates structural alterations in the atrium induced by Ang II with reduced inflammatory damage in the atrium in hypertensive models [9]. Depletion of platelets via anti-GP1ba antibody, blockade of platelet P-selectin, or inhibiting platelet with clopidogrel effectively limits the interaction between activated platelets and leukocytes, preventing cardiac remodeling in transverse aortic constriction (TAC)-induced hypertensive models [7]. Furthermore, platelet activation has been shown as an early event during hypertension induced by Ang II, stimulating the conjugation between platelets and leukocytes and promoting the recruitment of inflammatory cells into cardiac tissue, where they contribute to cardiac fibrosis by secreting inflammatory cytokines [10]. Consistent with this, several studies have emphasized platelets as a source of cytokines that may drive macrophage polarization toward a fibrogenic phenotype, thereby activating fibroblasts and promoting cardiac remodeling [11]. Nevertheless, how platelets contribute to Ang II-induced cardiac remodeling remains poorly defined, and the effector molecules triggering platelet activation in this context are not well characterized. Additionally, the potential cooperation between platelets and macrophages during the development of cardiac remodeling warrants further investigation.

C-C chemokine motif ligand 5 (CCL5), also known as RANTES, is a chemokine that regulates monocytes and T cells migration during various pathological processes [12, 13]. CCL5 is abundant in

platelet a-granules, and is secreted upon platelet activation [14]. Both CCL5 receptors, CCR1 and CCR3, are expressed on platelets [15]. However, the role of CCL5 on platelet function remains poorly understood. Substantial evidence suggests that CCL5 is implicated in inflammatory diseases, including viral infections, asthma, atherosclerosis, and liver fibrosis [16]. Pharmacological or genetic interventions targeting CCL5 attenuate the infiltration of T lymphocytes and macrophages into perivascular adipose tissue induced by Ang II, thereby enhancing vascular performance [17]. In contrast, CCL5 knockout (KO) mice exhibit exacerbated kidney damage compared to wild-type (WT) controls with Ang II infusion, which results from increased macrophage infiltration, heightened and pro-inflammatory cytokine production [18]. These observations reveal that CCL5 plays a complex and pivotal role in end-organ damage in hypertension. Given the central involvement of platelets in cardiovascular pathology and the significance of autocrine mechanisms in controlling platelet function, this study investigated whether CCL5 triggers platelet activation to influence hypertensive remodeling.

The present work clarifies the contribution of CCL5 to inflammatory responses mediated by platelets during cardiac remodeling induced by Ang II. The results elucidate a previously unrecognized pathway through which CCL5 activates platelets through CCR1 and CCR3 receptors to promote activation of nuclear factor-kappa B (NF-κB) signaling. This activation, subsequently, regulates the secretion of TGF-β1 derived from platelets, ultimately promoting the differentiation of macrophages towards the M2 phenotype. Additionally, CCL5 deficiency prevents platelet activation, platelet-driven M2 macrophage polarization, and cardiac remodeling in Ang II-infused mice. This work offers new perspectives on platelet biology, emphasizing how CCL5 enhances platelet activation and promotes a pro-fibrotic macrophage phenotype during hypertension-induced cardiac remodeling.

Materials and Methods

Experimental animals

The congenic CCL5 KO mice, male and 10–12 weeks old, were derived from the C57BL/6J strain using CRISPR/Cas9 technology targeting exons 1 to 3 of the CCL5 gene. A 5214 bp deletion, accompanied by a point mutation (G>A), was introduced in this region, resulting in a premature termination of translation. The positive founder was crossed into C57BL/6J mice to generate heterozygous individuals,

which were subsequently intercrossed to produce the CCL5 KO mice. Genotypes (Figure S1A) were confirmed *via* DNA sequencing of tail samples using the forward sequencing primer: GATAATAG ATGGACATAGAGGACACAACTC (Figure S1B). All animal protocols were reviewed and approved by the Animal Care and Use Committee at the Institute of Materia Medica, Chinese Academy of Medical Sciences & Peking Union Medical College, ensuring full adherence to the ARRIVE guidelines. (Approval no. 00003901).

Hypertensive mice model established via Ang II infusion

To induce hypertension, mice received a continuous infusion of angiotensin II (Ang II, Sigma-Aldrich, St. Louis, MO, USA) at a rate of 1500 ng kg⁻¹ min⁻¹ for 7 days [19]. Following assessment of hemodynamic parameters, mice were anesthetized with 2% isoflurane and euthanized. Isolated hearts were excised and processed for histological, RNA sequencing, and molecular analyses. All animals were assigned an alphanumeric designation for blinding purposes.

Aspirin (ASA) and clopidogrel (CPG) treatment

ASA (Sigma-Aldrich) and CPG (MedChemExpress, NJ, USA) were dissolved separately in 300 mL of drinking water (0.4 mg/mL ASA, 0.15 mg/mL CPG) and provided with free access for 24 hours [20]. The drinking water was replaced daily. Pre-treatment with ASA or CPG was initiated three days prior to the start of Ang II administration and maintained during the entire period of Ang II challenge.

Platelet depletion/reconstitution model

Busulfan model: Busulfan (HY-B0245, MedChemExpress), a selective bone marrow toxin, was used to induce platelet depletion [21]. On days 0 and 3, mice were administered busulfan (20 mg/kg) or vehicle intraperitoneally. After 14 days, washed platelets were injected intravenously into the platelet-depleted mice 20 minutes prior to Ang II infusion. The injection was repeated on day 3 post-surgery. The injection volume of 200 µL contained 5 × 10⁸ platelets. Busulfan administration did not significantly change the quantity of peripheral blood leukocytes, which was verified using flow cytometric analysis (Figure S2).

Antibody model: One intraperitoneal injection of a GPIb α -blocking antibody (0.3 $\mu g/g$, R300; Emfret Analytics, Bayern, Germany) was administered to the mice. After 24 hours, washed platelets were injected

intravenously into the platelet-depleted mice 20 minutes prior to Ang II infusion. The injection was repeated on day 3 post-surgery. The injection volume of 200 μ L contained 1 × 10 9 platelets.

Immunohistochemistry and immunofluorescence

Immunohistochemistry of cardiac sections was conducted with primary antibodies against α-SMA (1:200; ab5694, Abcam Cambridge, MA, USA), MAC-2 (1:200; ab76245, Abcam Cambridge), CD8 (1:1000; ab217344, Abcam Cambridge), CD163 (1:100; ab182422, Abcam Cambridge), and CD41 (1:50; sc-365938, Santa Cruz Biotechnology, CA, USA), ARG-1 (1:200; 16001-1-AP, Proteintech, Wuhan, China). A semiquantitative assessment of staining was performed, incorporating both intensity (0: none; 1: mild; 2: moderate; 3: intense) and the percentage of positive cells (0: 0%; 1: 1–25%; 2: 26–50%; 3: 51–75%; 4: 76-100%). Immunofluorescence of cardiac sections was conducted with primary antibodies against CCL5 (1:100; 710001, Sigma-Aldrich), CD41 (1:50; sc-365938, Santa Cruz Biotechnology), α-SMA (1:200; ab5694, Abcam Cambridge), iNOS (1:100; 18985-1-AP, Proteintech), ARG-1 (1:200; 16001-1-AP, Proteintech), CD68 (1:100; 38005, Signalway Antibody, Beijing, China), MAC-2 (1:200; ab76245, Abcam Cambridge), CD8 (1:500; ab217344, Abcam Cambridge), α-actin (1:200; A5044, Sigma-Aldrich), CD31 (1:200; 77699S, Cell Signaling Technology), and TGF-β1 (1:50, sc-130348, Santa Cruz Biotechnology; 1:100, ab92486, Abcam Cambridge). Cardiomyocyte cross-sectional area was detected by wheat germ agglutinin (WGA; Invitrogen, Waltham, MA, USA). Immunofluorescence of macrophages and platelets was performed with primary antibodies targeting CCR1 (1:100; 54526, Signalway Antibody), CCR2 (1:100; bs-0562R, Bioss, Beijing, China) and CCR3 (1:100; 56092, Signalway Antibody). Analysis was conducted with a confocal laser scanning microscope (Leica, Wetzlar, Germany).

Cardiac magnetic resonance imaging (CMRI)

CMRI studies were performed on mouse hearts using a 7.0 T Bruker BioSpec system (Bruker Medical, Ettlingen, Germany), which was fitted with a small animal coil. Short-axis cine images of the left ventricle were obtained. Throughout the cardiac cycle, fifteen phases were captured, acquiring continuous slices from the cardiac base to the apex. ParaVision 6.0.1 (Bruker BioSpec, Bruker Medical) was used for image analysis.

Blood pressure measurement

Arterial blood pressure was measured using a non-invasive tail-cuff system (Softron BP-98A, Tokyo,

Japan). Experiments were conducted in a quiet, darkened room (22 ± 2 °C), with access restricted to the operator during measurements. To minimize stress, mice were acclimated to the restraint tubes, and trained to voluntarily enter the restraint tubes during measurement. Mice were subjected to a standardized warming protocol of 35°C for 5 minutes prior to data acquisition and were maintained at this temperature throughout the measurement period. Following an initial warm-up period of 10 cycles, data from the subsequent 5 to 15 cycles (of a total 15-25) per session were retained for analysis, and these cycles were used to calculate average blood pressure for statistical comparisons. To ensure measurement accuracy and reliability, mice were acclimated to the tail-cuff procedure through a training period of at least five consecutive days prior to experimental data collection.

RNA sequencing analysis

RNA sequencing of ventricular tissue was conducted by an Illumina HiSeq4000 system (Expandbio, Beijing, China). PCA analysis was conducted using the scatterplot3d in R to reveal the interrelationship between the samples. Differentially expressed genes (DEGs) were discerned between saline-treated WT and Ang II-infused WT hearts, as well as between Ang II-treated WT and Ang II-infused CCL5 KO hearts, via the 'limma' package in R, considering an adjusted P-value < 0.05 as The statistically significant. R-based "clusterProfiler" was employed to conduct KEGG, GO, along with GSEA, regarding an FDR-adjusted P-value below 0.05 as significant. Immune infiltration was evaluated with five different methods: murine Microenvironment Cell Population (mMCP-counter) [22], Estimating the Proportion of Immune and Cancer Cells (EPIC) [23], Tumor Immune Estimation Resource (TIMER) [24, 25], Tumor Immune contexture from human RNA-seq data (quanTIseq) [26], and Celltype Identification By Estimating Relative Subsets of RNA Transcripts (CIBERSORT-ABS) [27].

GEO dataset analysis

RNA-seq datasets for both control and Ang II-infused groups (16 samples per group) were acquired from the Gene Expression Omnibus (GEO) repository (GSE261273 and GSE261275). DEGs were determined using a corrected P-value threshold of 0.05. Correlations in transcript levels were assessed using Spearman's method, considering a P-value below 0.05 and an absolute correlation coefficient exceeding 0.3 as statistically significant.

Molecular docking analysis

To explore the binding between CCL5 and its receptors CCR1 and CCR3, rigid protein-protein docking was carried out with ZDOCK. The three-dimensional structures of CCL5, CCR1, and CCR3 were acquired from the Protein Data Bank (PDB). Protein-protein interactions were examined and visualized using PyMol (Version 2.4).

Platelet isolation

Cardiac puncture was performed to collect whole blood into acid-citrate-dextrose (1:7). Platelet rich plasma was obtained via centrifugation for 11 minutes at 200 g and room temperature. After washing with two rounds of CGS solution containing PGE1 (1 μ M; HY-B0131, MedChemExpress), platelets were finally suspended in a modified Tyrode's solution to a density of 3 \times 108/mL. Platelets were allowed to recover to a resting state by incubating at room temperature for 1 hour.

Spreading of platelets

Fibrinogen (10 μg/mL; HY-125864, Sigma-Aldrich) was applied to cell culture plates with glass coverslips overnight at 4°C. The platelets were left for two hours at 37°C to allow adhesion and spreading on the fibrinogen-coated surfaces. After fixation and permeabilization, attached platelets were stained with FITC-labeled phalloidin (CA1620, Solarbio, Beijing, China). Confocal laser scanning microscopy (Leica) was used to capture images, and ImageJ software was used to calculate each platelet's spreading area.

Flow cytometry

Washed platelets were incubated with FITC anti-mouse CD41 antibody (133904; Biolegend, San Diego, CA, USA) and APC anti-mouse/rat CD62P (148304; Biolegend) for 15 minutes. In inhibitor experiments, washed platelets were pre-treated with or without aspirin (2 mM; A2093, Sigma-Aldrich), BAY 11-7082 (1 μM; HY-13453, MedChemExpress), CCR1 blocking antibody (50 µg/mL, K115510P-Ag, Solarbio, Beijing, China) or CCR3 blocking antibody (50 μg/mL, K113920P-Ag, Solarbio, Beijing, China) for 15 minutes before stimulation with or without rmCCL5 (100 ng/mL; 250-07, PeproTech) in the presence of ADP (5 µM; A2754, Sigma-Aldrich) for 10 minutes. The specificity of blocking antibodies was confirmed using both bone marrow-derived macrophages (BMDMs) and platelets (Figure S3). BMDMs treated with CCR1 and CCR3 blocking antibodies were stained with APC anti-mouse CCR1 (152503), PE/Cyanine7 anti-mouse CCR2 (150611) and APC anti-mouse CCR3 (144511) (all from Biolegend) for 30 minutes at 4 °C.

For peripheral blood leukocyte subsets quantification, 100 μ L of peripheral blood was stained with the following antibodies: PE/DazzleTM 594 anti-CD45 (103146), PE anti-CD11b (101208), APC anti-F4/80 (157305), FITC anti-Ly-6G (127605), PE anti-CD3 (155608), APC anti-CD4 (100516), FITC anti-CD8a (100706), and APC anti-CD19 (115512) (all from BioLegend). Then erythrocytes were lysed by incubating the samples with 1 mL of BD FACS lysing solution (349202; BD Biosciences, San Jose, CA, USA) per 100 μ L of blood.

To identify cardiac macrophage subpopulations, mice were euthanized and hearts were perfused with heparinized saline (2% heparin) to clear residual blood. Cardiac tissues were dissociated enzymatically using a mixture of dispase II (2.4 U/mL) and collagenase type II (0.01 mg/mL) for 60 minutes at 37 °C. The resulting single-cell suspensions were sequentially filtered through 70-µm and 40-µm strainers. To minimize nonspecific antibody binding, cells were pre-blocked with an anti-CD16/32 antibody and subsequently stained with a Fixable Viability Dve and fluorescently labeled antibodies: PE/Dazzle™ 594 anti-mouse CD45 (103146), APC anti-mouse F4/80 (157305), PE anti-mouse CD86 (105008), and PE/Cyanine7 anti-mouse CCR2 (150611) (all from BioLegend). Following washing and centrifugation, cells were fixed, permeabilized, and stained with FITC anti-mouse CD206 (141703; BioLegend).

ImageStream Mark II imaging flow cytometry (Amnis, EMD-Millipore, Seattle, WA, USA) was used for sample analysis, and IDEAS statistical image analysis software (Amnis, EMD-Millipore, Seattle, WA, USA) was used for data processing.

Bone marrow-derived macrophages (BMDMs)

Bone marrow cells were flushed from femurs and tibias with DMEM using a 1 mL syringe and then isolated via Ficoll-Paque density gradient centrifugation. Macrophages were polarized from bone marrow cells treated with 10 ng/mL M-CSF (PeproTech) for 3 days, and proliferated in new media for another 2 days before use for experiments [3]. BMDMs were co-cultured with wild-type (WT) or CCL5 knockout (KO) mouse-derived platelets at a ratio of 1:1000, along with ADP (10 µM) and Ang II (100 nM) for 48 hours. Polarization toward the M2 phenotype was evaluated using immunofluorescence and real-time PCR. Culture supernatants were collected for subsequent fibroblast stimulation experiments.

Generation of M1 and M2 macrophages

RAW264.7 cells were polarized into M1 macrophages through stimulation with (LPS, lipopolysaccharide 100 ng/mL; L2880, Sigma-Aldrich) and interferon-gamma (IFN-v, 20 ng/mL; AF-315-05, PeproTech). For M2 polarization, cells were treated with IL-4 (20 ng/mL; AF-214-14, PeproTech) and IL-13 (20 ng/mL; 210-13, PeproTech), while control groups (M0) received only culture medium. All treatments were carried out for 48 hours in vitro.

Cardiac fibroblasts

brief, heart tissues from neonatal Sprague-Dawley rats were minced and subjected to sequential digestions in a solution of 0.1% trypsin and 100 U/mL collagenase type II at 37 °C. Filtration was performed on the supernatant using a 70-um cell strainer. The final resuspended cells were plated for 90 minutes to facilitate fibroblast adhesion. Before subsequent experiments, cells were cultured in DMEM with 5% FBS for 24 hours. To induce myofibroblast differentiation, cells were stimulated by conditioned media from M1 macrophages, M2 macrophages, or platelet-educated BMDMs for 48 Differentiation assessed hours. was via immunofluorescence and RT-PCR.

Enzyme-linked immunosorbent assay (ELISA)

TGF- $\beta1$ levels were detected using a Mouse TGF- $\beta1$ pre-coated ELISA kit (1217102; DARKEWE, Shenzhen, China) or a Rat TGF- $\beta1$ ELISA kit (ERC107b.48; Neobioscience Technology Co, Ltd., Shenzhen, China).

Western blotting analysis

SDS-PAGE of 10%, 15%, or 20% was used for protein separation. Primary antibodies against CCL5 (1:1000; 710001, Sigma-Aldrich), MRC-1 (1:1000; ab646963, Abcam, Cambridge, MA, USA), TGF-β1 (1:500; sc-130348, Santa Cruz Biotechnology), P65 (1:1000; 8242T, Cell Signaling Technology, Danvers, MA, USA), p-P65 (1:1000; 11014, Signalway Antibody, Beijing, China), and GAPDH (1:1000; 5174s, Cell Signaling Technology) were used. Protein signals were visualized by enhanced chemiluminescence (ECL; P90720, EMD-Millipore, Seattle, WA, USA) following incubation with species-matched secondary antibodies, and images were acquired using an ImageQuant™ LAS 4000 system (GE, Boston, USA).

Real-time PCR (RT-PCR)

The commercial RNA Tissue/Cell Rapid Extraction Kit (Shandong Sparkjade Biotechnology Co., Ltd., China) was used for total RNA extraction.

Reverse transcription was conducted with SPARKscript II RT Plus Kit (Shandong Sparkjade Biotechnology Co., Ltd.). Quantitative PCR was performed using SPARKscript II SYBR One Step qRT-PCR Kit (Shandong Sparkjade Biotechnology Co., Ltd.) and specific primers on an Applied Biosystems 7900 PCR system (ABI, Carlsbad, CA, USA) (Table S1). 2-AACt method was used for RNA expression analysis with GAPDH as the endogenous reference gene.

Statistical analysis

Data were presented as mean ± SD. The distribution of data was assessed by Shapiro-Wilk normality test. For normally distributed data, Student's t-test was applied for two-group comparisons, and one-way ANOVA followed by Tukey's post-hoc test was used for comparisons between three or more groups. For non-normally distributed variables, Mann-Whitney test was applied for comparisons between two groups, while the Kruskal-Wallis test with Dunn's post hoc analysis was applied for comparisons among multiple groups. (*p < 0.05, **p < 0.01, ***p < 0.001, NS indicating no significant difference).

Results

CCL5 deficiency attenuated Ang II-promoted cardiac fibrosis, hypertrophy, and dysfunction

To evaluate the contribution of CCL5 to Ang II-induced cardiac remodeling, chemokine gene expression was assessed in cardiac tissue from Ang II-infused mice at day 7. Two mRNA sequencing datasets (GSE261273 and GSE261275) were retrieved from the GEO database, comprising a total of 32 samples – 16 from saline-treated controls and 16 from Ang II-infused animals [28]. Of the 29 chemokine genes examined, Ccl5 showed the most marked induction in cardiac tissue following Ang II infusion when compared to sham-treated animals (Figure 1A), highlighting its central role in cardiac remodeling processes driven by Ang II. Pathway enrichment and gene set enrichment analysis (GSEA) based on GEO datasets revealed multiple signaling pathways regulating CCL5 expression were activated in Ang II-infused heart (Figure S4A). These pathways included the mitogen-activated protein kinases (MAPK), Janus kinase/signal transducer activator of transcription (JAK-STAT), nuclear factor-kappa B (NF-κB), and the phosphatidylinositol 3-kinase (PI3K)/Akt signaling pathway [29-31]. A strong positive correlation between the scores of these pathways and Ccl5 gene expression demonstrated by gene set variation analysis (GSVA)

(Figure S4B). The upregulation of CCL5 protein in Ang II-infused hearts was subsequently confirmed through both immunofluorescence and western blotting analysis (Figure 1B, C).

To evaluate the functional role of CCL5 in Ang II-induced hypertensive cardiac remodeling, wild-type (WT) and CCL5 knockout (CCL5 KO) mice were examined. Quantitative PCR measurements verified elevated cardiac Ccl5 transcript levels in WT mice following Ang II infusion, while confirming its absence in CCL5 KO animals (Figure 1D). Genetic deletion of CCL5 did not alter hypertension triggered by Ang II (Figure S5). Histological evaluation with Masson's trichrome revealed that CCL5 KO markedly reduced both perivascular and interstitial fibrosis induced by Ang II, along with a decrease in α -smooth muscle actin (a-SMA)-positive myofibroblast accumulation (Figure 1E, F). Cardiac hypertrophy promoted by Ang II, assessed via cardiomyocyte cross-sectional area, was also significantly suppressed in CCL5 KO mice (Figure 1G). Furthermore, mRNA expression of fibrotic hypertrophic and markers—collagen I (Col1a1), collagen III (Col3a1), atrial natriuretic factor (Anf), and brain natriuretic peptide (Bnp)-was notably lower in CCL5 KO compared to WT mice after Ang II challenge (Figure 1H, I). Cardiac MRI assessments indicated that CCL5 deficiency alleviated Ang II-impaired contractility, reflected by recovered left ventricular ejection fraction (EF%) and fractional shortening (FS%), as well as reduced end-systolic anterior and posterior wall thicknesses relative to WT mice (Figure 1J). Taken together, these data indicate a critical function for CCL5 in driving Ang II-induced cardiac fibrosis, hypertrophy, and ventricular dysfunction.

Transcriptomic profiling reveals CCL5-mediated regulation in hypertensive cardiac remodeling

To uncover the transcriptional mechanisms through which CCL5 deficiency confers protection against hypertensive cardiac remodeling, we carried out RNA-seq on heart tissues from WT and CCL5 KO mice following infusion with saline or Ang II. Principal component analysis (PCA) illustrated clear all separation among groups, with high reproducibility within replicates and condition-specific transcriptomic signatures (Figure 2A). Ang II challenge led to substantial transcriptional activation in WT hearts, which was markedly reduced in CCL5 KO mice, implying that CCL5 loss restrains Ang II-induced gene expression changes (Figure 2B). GSEA was employed to identify processes modulated by CCL5. In WT animals, Ang II stimulation enriched pathways related to immune chemotaxis, extracellular

matrix (ECM) organization, complement coagulation systems, platelet function, NF-κB signaling, and T cell activation-effects that were diminished in CCL5-deficient mice under Ang II treatment (Figure 2C and Figure S6A, B). Conversely, both saline-treated WT and CCL5 KO Ang II groups displayed enrichment in metabolic pathways governing carbohydrates, amino acids, and lipid metabolism (Figure S6C, D). Further validation through KEGG and GO term analyses corroborated that Ang II elevated expression of pro-inflammatory genes, ECM regulators, platelet activators, NF-kB, and TGF-β signaling components, while repressing metabolic genes. These effects were substantially reversed in CCL5 KO mice (Figure 2D-G, S6E, F). To further elucidate the role of CCL5 in Ang II-activated

biological processes and signaling pathways, correlation analysis was performed on 32 heart RNA-sequencing datasets from the GEO database (GSE261273 and GSE261275) [28]. Ccl5 expression showed a strong positive correlation with the signature genes involved in platelet activation, NF-κB, and TGF-beta signaling pathways (Figure 2H-J). Additionally, gene set variation analysis (GSVA) scores of these pathways also showed a robust positive correlation with Ccl5 gene expression (Figure 2K). Collectively, these results confirm CCL5 deficiency protects from hypertensive cardiac fibrosis through reduced ECM deposition and suggest that the underlying mechanism involves the inhibition of platelet activation, TGF-beta signaling, and NF-kB signaling pathways.

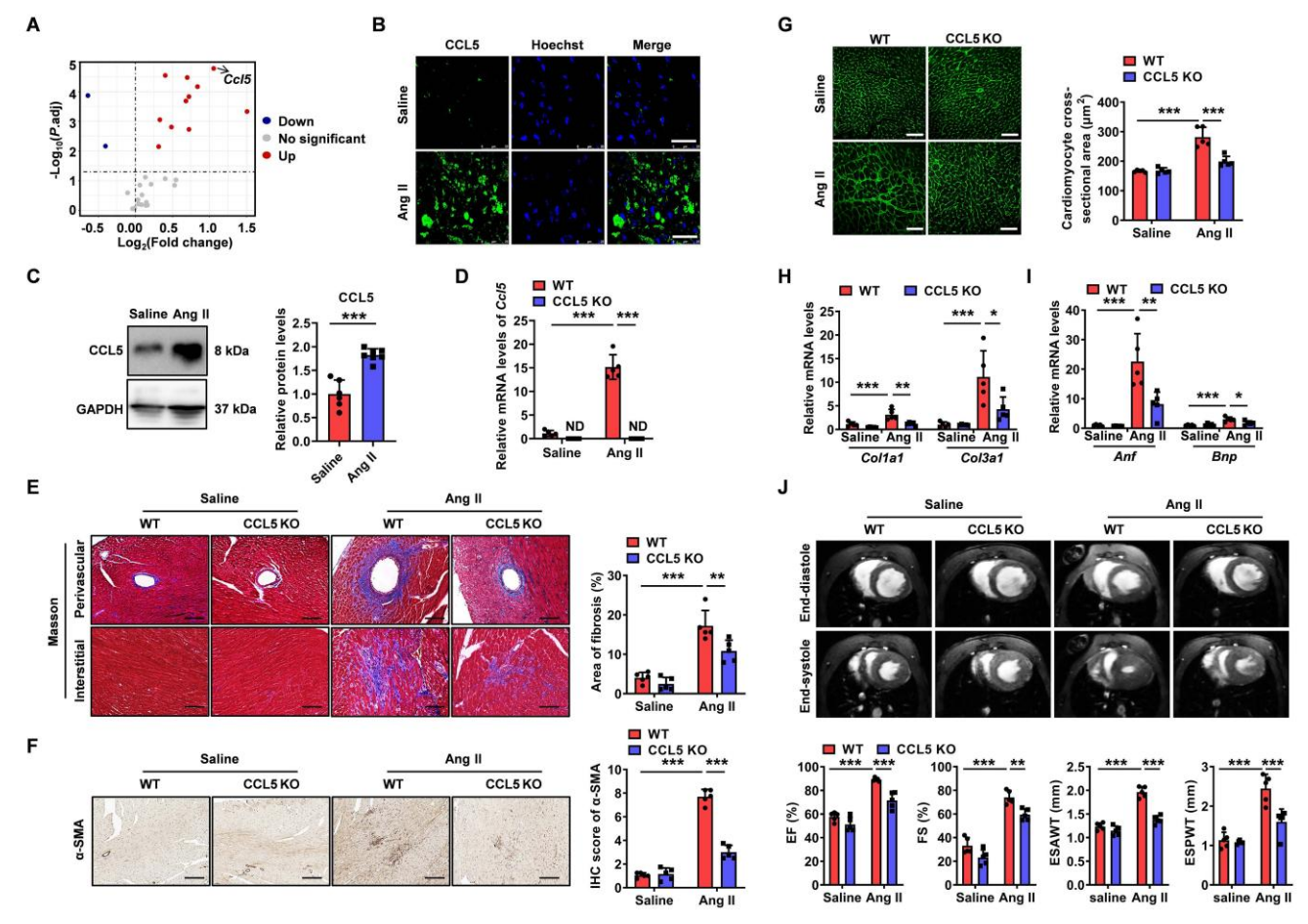


Figure 1. CCL5 deficiency attenuated Ang II-promoted cardiac fibrosis, hypertrophy, and dysfunction. Fold change and statistical analysis of chemokine transcript levels in hearts exposed to angiotensin II (Ang II), compared with saline-treated controls at day 7, based on GEO datasets (n = 16 per group). Wild-type (WT) mice received a 7-day infusion of either saline or Ang II. B CCL5 (green) in the heart detected by immunofluorescence (n = 5; Scale bar: 25 μm). C CCL5 protein levels in the hearts detected by western blotting analysis of (n = 6 for saline and n = 7 for Ang II groups). WT and CCL5 KO mice were subjected to a 7-day infusion of saline or Ang II (n = 5 per group). D The gene expression of Ccl5 in heart tissues assessed by RT-PCR. E Myocardial fibrosis detected by Masson's trichrome staining (Scale bar: 100 μm). F Immunohistrochemistry of α-SMA in the heart (Scale bar: 100 μm). G FITC-WGA staining showed cardiomyocyte cross-sectional area (Scale bar: 50 μm). H, I Genes expression of Col1a1, Col3a1, Anf, and Bnp in heart tissues. J CMRI analysis of left ventricle at end-systole and end-diastole. Data are presented as mean ± standard deviation, with n representing the number of animals. * P < 0.05, *** P < 0.01, **** P < 0.01, ND indicating no detection and NS indicating no significance.

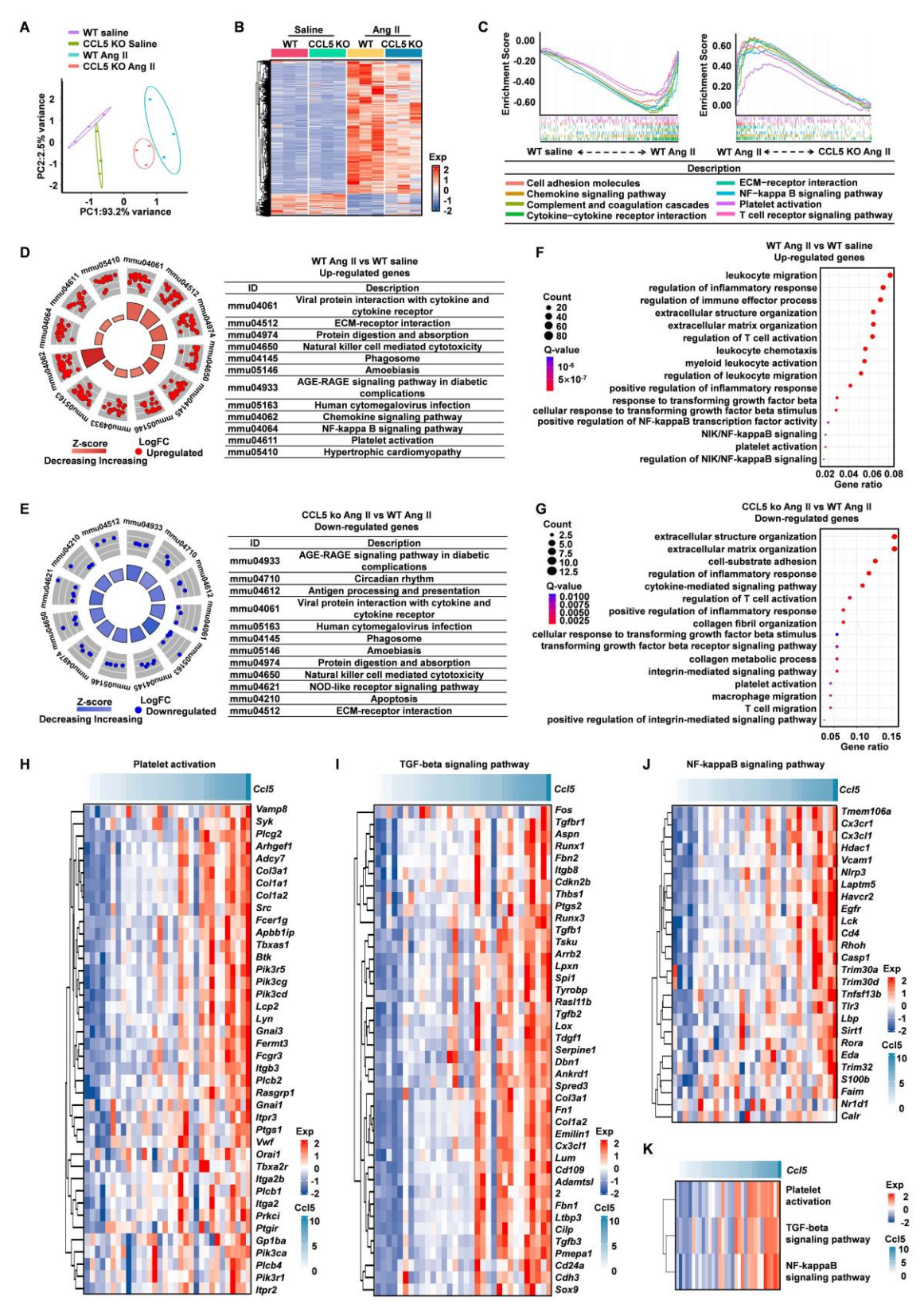


Figure 2. Transcriptomic profiling reveals CCL5-mediated regulation in hypertensive cardiac remodeling. Cardiac tissues from WT and CCL5 KO mice infused for 7 days with saline or Ang II were analyzed *via* RNA sequencing (n = 3 per group). A Principal component analysis (PCA) illustrating distinct transcriptomic profiles among the four experimental groups. B Heatmap of differentially expressed genes (DEGs) identified in WT Ang II vs. WT saline hearts, and in CCL5 KO Ang II vs. WT Ang II hearts. C Gene Set Enrichment Analysis (GSEA) highlighting biological pathways enriched in WT Ang II hearts relative to both saline-treated WT and CCL5 KO Ang II groups. D, E KEGG pathway analysis of up-regulated genes under Ang II stimulation in WT mice (D) and down-regulated genes in CCL5 KO Ang II vs. WT Ang II hearts (E). F, G Significantly enriched Gene Ontology (GO) terms for up-regulated genes in WT Ang II vs. saline controls (F) and down-regulated genes in CCL5 KO Ang II vs. WT Ang II hearts (G). H–J Correlation analysis in WT mice between Cd5 expression and key genes involved in platelet activation, TGF-β, and NF-κB signaling under Ang II or saline conditions (GEO datasets; n = 32). K Correlation of Cd5 transcript levels with Gene Set Variation Analysis (GSVA) scores for platelet activation, TGF-β, and NF-κB pathways following Ang II or saline infusion (n = 32).

CCL5 deficiency reduces platelet activation to attenuate Ang II-promoted cardiac remodeling

RNA sequencing revealed that CCL5 deficiency dampened Ang II-induced platelet-associated gene expression, likely due to reduced platelet infiltration or diminished platelet activation (Figure 3A). To further identify the impact of CCL5 on platelet deposition in hypertensive cardiac remodeling, immunofluorescence for CD41 was performed on heart tissues. Ang II infusion significantly increased platelet accumulation, with the accumulated platelets (CD41) predominantly localized with the fibrotic areas (α-SMA) in WT Ang II hearts. This platelet accumulation was markedly reduced in CCL5 KO hearts (Figure 3B). Platelet activation was assessed by measuring the release of P-selectin from platelet α-granules, indicated by surface CD62P expression. CCL5 KO significantly reduced CD62P-positive peripheral blood (Figure platelets in Additionally, imaging flow cytometry of platelets stimulated with ADP in vitro revealed a decrease in α-granule release in the absence of CCL5 (Figure 3D). Platelet spreading upon thrombin stimulation was also reduced in CCL5 KO mice (Figure 3E). RT-PCR analysis showed that Ccr1 and Ccr3 gene expression in washed platelets was unaffected by CCL5 deficiency (Figure 3F). The interactions of CCL5 with CCR1 and CCR3 were confirmed by molecular docking analysis (Figure S7). Furthermore, recombinant CCL5 (rmCCL5) directly enhanced platelet α-granule release and spreading (Figure 3G, H). These results suggest that CCL5 deficiency not only reduces platelet accumulation in Ang II-infused hearts but also directly suppresses platelet activation, without altering the expression of CCL5 receptors on platelets.

To assess whether platelet activation inhibition is critical for the protection of CCL5 deficiency in cardiac injury, platelet inhibitors, including aspirin (ASA) and clopidogrel (CPG), were administered to WT and CCL5 KO mice infused with Ang II. As anticipated, both ASA and CPG significantly mitigated cardiac fibrosis and hypertrophy in Ang II-infused WT mice (Figure 3I, J). However, no additional protective effects were observed in CCL5 KO mice infused with Ang II (Figure 3I, J). The direct effects of ASA on rmCCL5-stimulated platelets were then evaluated. ASA was found to completely abolish the rmCCL5-induced upregulation of platelet surface CD62P expression and platelet spreading (Figure 3K, L). These results confirm that CCL5 modulates platelet activation to promote hypertensive cardiac remodeling.

CCL5 deficiency attenuates Ang II-promoted cardiac inflammation

To investigate the impact of CCL5 deficiency on II-promoted cardiac inflammation, deconvolution algorithms were employed to analyze RNA-sequencing data, revealing the immune cell infiltration profile in WT and CCL5 KO hearts with or without Ang II stimulation. The accumulation of various immune cell types observed in Ang II-infused WT hearts was notably reduced by CCL5 KO (Figure including S8A), memory cells. macrophages/monocytes, cancer-associated fibroblasts, CD8+ T cells, myeloid dendritic cells, M2 macrophages, regulatory T cells, and NK cells. Among these, the distribution of CD8+ T cells (EPIC, TIMER, and CIBERSORT-ABS), macrophages (mMCPCounter and TIMER), and M2 macrophages (QUANTISEQ and CIBERSORT-ABS) was confirmed by two or more algorithms (Figure 4A and Figure S8A, B). Pathological staining corroborated the reduction of CD8+ T cells and macrophages in Ang hearts CCL5 KO (Figure RNA-sequencing revealed the downregulation of gene markers for pro-inflammatory M1 pro-fibrotic M2 macrophages in Ang II-infused CCL5 KO hearts compared to WT hearts, a finding confirmed by RT-PCR (Figure 4C, D). Compared to M1 macrophages, M2 macrophages exhibit a more pronounced capacity to stimulate myofibroblast differentiation. This was demonstrated by the observation that supernatants from M2 macrophages significantly increased the protein levels of α-SMA and the gene expression of Sm22, Col1a1, and Col3a1 in cardiac fibroblasts, relative to supernatants from M1 macrophages (Figure S9). The majority macrophages in Ang II-infused WT hearts highly expressed the M2 macrophage marker ARG-1, while only a small fraction exhibited high expression of the M1 macrophage marker iNOS, indicating a more critical role for M2 macrophages in Ang II-induced cardiac remodeling and inflammation (Figure 4E-G). CCL5 KO significantly attenuated the Ang II-induced increase in both the abundance and proportion of M2 macrophages in the heart (Figure 4E and G). Although the quantity of iNOS-expressing M1 macrophages in the heart was reduced in CCL5 KO mice compared to WT mice in response to Ang II, the proportion of M1 macrophages remained comparable between the two groups (Figure 4F and G). Cardiac macrophage subpopulations were further investigated using flow cytometic analysis. The overall abundance of macrophages within total cardiac cells significantly reduced in CCL5 KO mice (Figure S10).

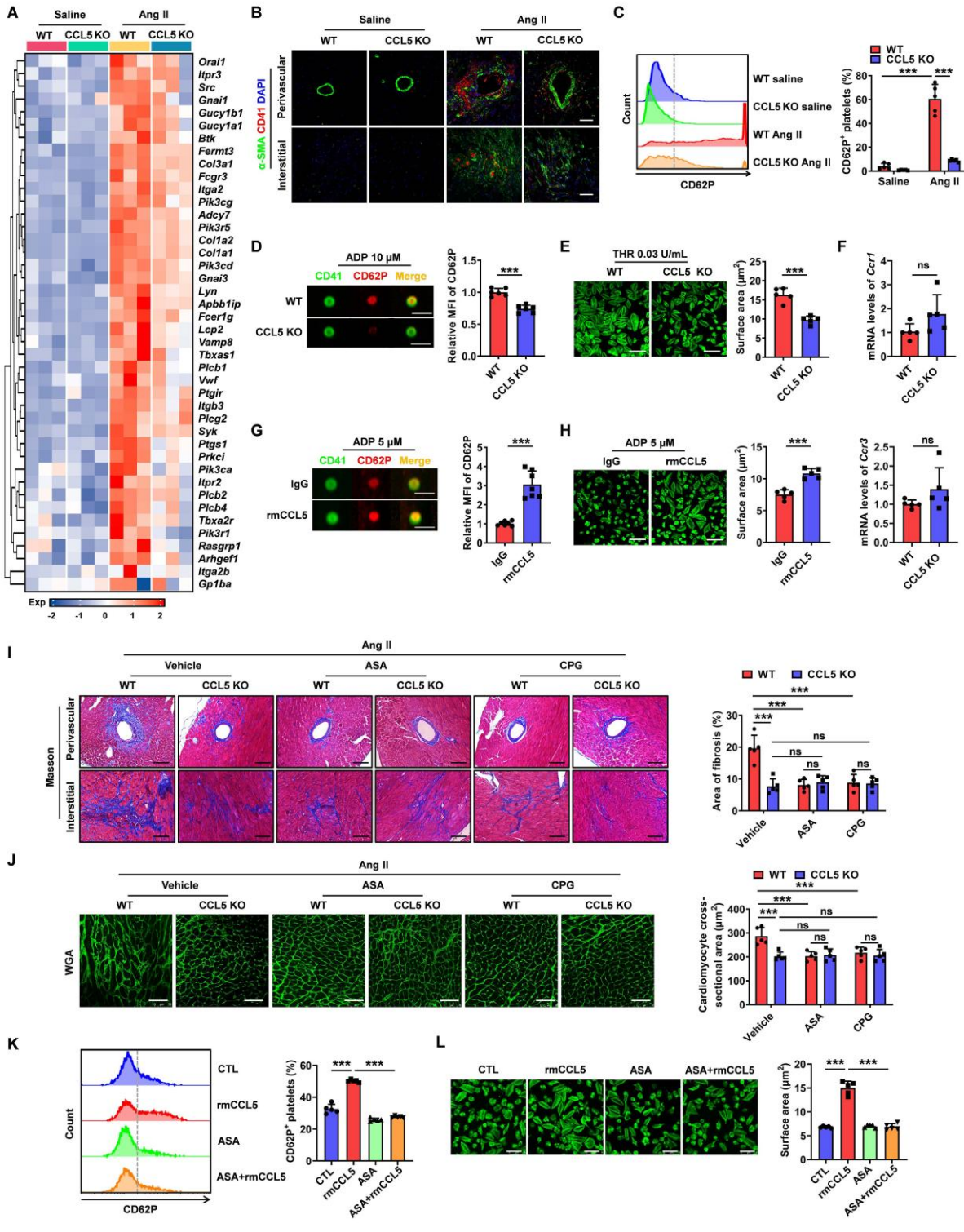


Figure 3. CCL5 deficiency reduces platelet activation to attenuate Ang II-promoted cardiac remodeling. WT and CCL5 KO mice were treated with saline or Ang II for 7 days. A Expression matrix data of platelet-associated genes in heart tissues, as detected by RNA sequencing (n = 3). B Immunofluorescence of platelets (red) and myofibroblasts (green) in the heart (n = 5; Scale bar: 50 μm). C Flow cytometry analysis of CD62P expression on circulating platelets in blood (n = 5). D Washed platelets from WT and CCL5 KO mice were activated by ADP (10 μM) for 10 minutes *in vitro*. The expression of CD62P was assessed by imaging flow cytometry (n = 6; Scale bar: 7 μm). E Washed platelets isolated from WT and CCL5 KO mice were stimulated with thrombin (THR, 0.03 U/mL) for 10 min prior to spreading on fibrinogen-coated wells for 2 h. Representative images of platelet spreading and quantification of spread area (μm²) are shown (n = 5; Scale bar: 10 μm). F Expression of Ccr1 and Ccr3 genes in platelets (n = 5). WT platelets stimulated by recombinant CCL5 (rmCCL5, 100 ng/mL) in the presence of ADP (10 μM) for 10 minutes *in vitro*. G Imaging flow cytometry analysis of CD62P expression (n = 7; Scale bar: 7 μm). H Representative images of platelet spreading and quantification of spread area (μm²) (n = 5; Scale bar: 10 μm). WT and CCL5 KO mice were infused with saline or Ang II for 7 days and treated with or without aspirin (ASA, 0.4 mg/mL) or clopidogrel (CPG, 0.15 mg/mL) in their drinking water (n = 5 per group). I Masson's trichrome staining of myocardial fibrosis (Scale bar: 100 μm). J WGA staining illustrating cardiomyocyte cross-sectional area (Scale bar: 50 μm). Washed platelets from WT mice were pretreated with or without ASA (2 mM) for 15 min, then stimulated with rmCCL5 (100 ng/mL) in the presence of ADP (10 μM) for 10 min *vitro*. K The percentage of CD62P-positive platelets was determined by flow cytometry analysis (n = 5). L Representative images of platelet spreading and quantification of platelet spread area (μm²)

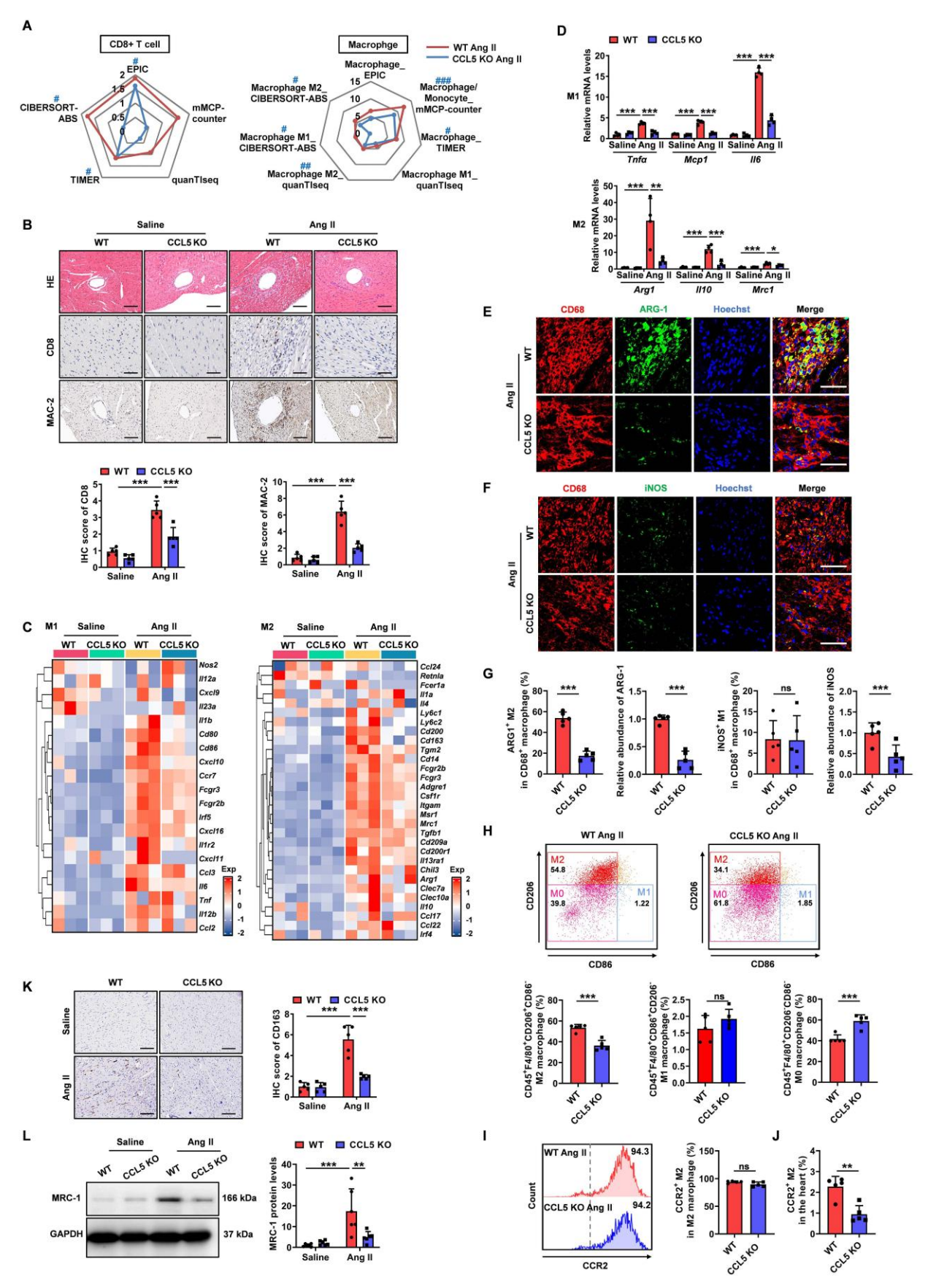


Figure 4. CCL5 deficiency attenuates Ang II-promoted cardiac inflammation. WT and CCL5 KO mice were subjected to a 7-day infusion of saline or Ang II. A Radar plot illustrating the extent of CD8+ T cells and macrophages, including M1 and M2 phenotypes, comparing CCL5 KO Ang II hearts to WT Ang II hearts using five algorithms (n = 3; # P adj < 0.05, ## P adj < 0.01, ### P adj < 0.01, ### P adj < 0.001 represents the CCL5 KO Ang II group compared to the WT Ang II group, with downregulation in blue). **B** HE staining and immunohistochemical staining of CD8+ T cells and macrophages (MAC-2 positive) (n = 5; Scale bar: 100 μ m for HE and MAC-2, 50 μ m for CD8). **C** Enrichment map of genes

related to M1 and M2 macrophage phenotypes detected by RNA-sequencing (n = 3). **D** RT-PCR detection of M1 ($Tnf\alpha$, Mcp1, and Il6) and M2 (Arg1, Il10, and Mrc1) macrophage markers (n = 4). Immunofluorescence of CD68 (red), ARG-1 (green) (**E**) and iNOS (green) (**F**) in the heart (n = 5; Scale bar: 50 µm). **G** The abundance and proportion of ARG-1* M2 and iNOS* M1 macrophage were quantified. **H** Flow cytometry analysis of M2 macrophage (CD45*F4/80*CD206*CD86*), M1 macrophage (CD45*F4/80*CD206*CD86*) in the hearts after Ang II infusion. The proportion relative to cardiac macrophages was quantified (n = 5). Flow cytometry analysis of CCR2* M2 macrophages was quantified (n = 5). **K** Immunohistochemical staining of CD163 in the hearts. (n = 5; Scale bar: $100 \, \mu$ m). **L** Western blotting analysis of MRC-1 protein levels in the hearts (n = 6). Data are presented as the mean \pm standard deviation, with n representing the number of animals. *P < 0.05, **P < 0.01, **** P < 0.001.

Among cardiac macrophages in Ang II-infused WT hearts, the predominant subset was M2 macrophages (CD206+CD86-), the proportion of which was decreased in CCL5 KO hearts (Figure 4H). In contrast, the percentage of M1 macrophages (CD86+CD206-) showed no significant change, while that of M0 macrophages (CD206-CD86-) was increased in CCL5 KO hearts (Figure 4H). In both WT and CCL5 KO hearts, M2 macrophages were predominantly CCR2+, with no significant difference in the CCR2+ proportion within the M2 subpopulation (Figure 4I). However, the relative proportion of CCR2⁺ M2 macrophages among total cardiac cells was reduced in CCL5 KO mice compared to WT mice (Figure 4J). These findings suggest that CCL5 modulates cardiac M2 macrophage abundance primarily through regulating the recruitment of circulating monocytes. Additionally, immunohistochemical staining showed that the Ang II-induced CD163-positive M2 macrophages in WT hearts was significantly diminished in CCL5 KO hearts (Figure 4K). Western blotting further confirmed the reduction in M2 macrophage mannose receptor 1 (MRC-1) expression in CCL5 KO hearts in response to Ang II (Figure 4L). These results indicate that CCL5 deficiency alleviates Ang II-promoted cardiac inflammation, specifically by reducing the accumulation of CD8+ T cells and macrophages, particularly pro-fibrotic macrophages.

CCL5-deficient platelets attenuate Ang II-promoted cardiac remodeling by suppressing M2 macrophage polarization

Numerous studies have demonstrated that platelets play a critical role as both initiators and amplifiers of the inflammatory response, actively engaging in immune cell recruitment and activation [6]. In this study, impaired platelet function and reduced immune cell infiltration were observed in Ang II-infused CCL5 KO mice compared to WT controls. To ascertain whether the suppressed platelet function stemming from CCL5 deficiency contributed to the attenuation of cardiac remodeling and inflammation, distinct two platelet depletion/reconstitution models were employed. In the first model, recipient mice underwent platelet depletion via administration of the chemotherapeutic agent busulfan. In the second, platelet depletion was achieved through the use of a specific anti-platelet

antibody. Subsequently, these platelet-depleted mice were reconstituted with either WT or CCL5 KO platelets. Platelet counts were assessed before depletion, after depletion, and after reconstitution to confirm successful depletion and reconstitution (Figure S11). Subsequently, hypertension was induced by 7-day Ang II infusion. In both platelet depletion/reconstitution models, WT reconstituted with CCL5 KO platelets exhibited reduced cardiac fibrosis, myofibroblast differentiation cardiomyocyte hypertrophy than reconstituted with WT platelets (Figure 5A-C). Histological analysis confirmed fewer CD41-positive platelets in the hearts of WT mice receiving CCL5 KO platelets compared to those receiving WT platelets (Figure 5D, E). Additionally, reconstitution with CCL5 KO platelets resulted in a significant reduction in the Ang II-induced infiltration of CD8+ T cells, macrophages, and M2 macrophages in the hearts of WT mice (Figure 5D, E). The reduction in fibrosis, inflammation, and M2 macrophage gene expression in CCL5 KO platelet-reconstituted WT mice in busulfan-induced platelets depletion model was validated RT-PCR further by (Figure Conversely, reconstitution of CCL5 KO mice with WT platelets resulted in similar pathological changes in response to Ang II, comparable to WT mice reconstituted with WT platelets, across both busulfan and antibody-induced platelet depletion models (Figure 5A-E). This suggests that CCL5 deficiency in non-platelet cell types does not reverse Ang II-promoted cardiac remodeling and inflammation, highlighting the essential role of impaired platelet function resulting from CCL5 deficiency in attenuating these processes.

To further examine the role of platelet CCL5 deficiency on M2 macrophage polarization within the heart, we assessed cardiac macrophage composition. Immunofluorescence staining revealed reconstitution with CCL5 KO platelets significantly decreased the proportion of M2 macrophages in Ang II-infused WT hearts, while exerting no significant effect on the proportion of M1 macrophages (Figure 6A-D). However, reconstitution of CCL5 KO mice with WT platelets exhibited similar cardiac macrophage composition in response to Ang II, as compared to WT mice reconstituted with WT platelets, in both the busulfan and antibody-induced platelet depletion mouse models (Figure 6A-D).

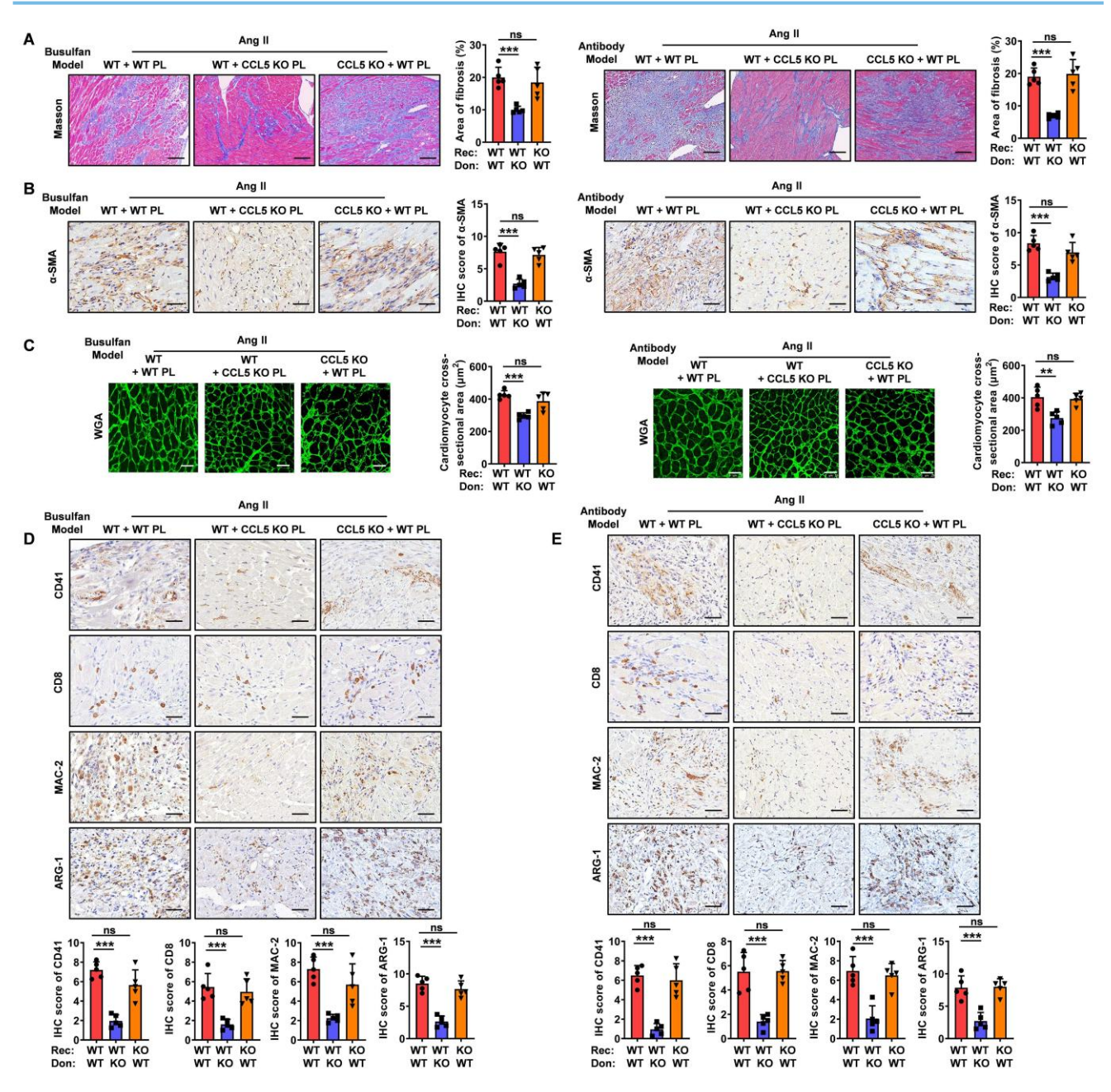


Figure 5. CCL5-deficient platelets attenuate Ang II-promoted cardiac remodeling by suppressing M2 macrophage polarization. Two distinct platelet depletion models: one induced by the chemotherapeutic agent busulfan (busulfan model) and another by a specific anti-platelet antibody (antibody model) were established. The platelet-depleted mice were reconstituted with platelets derived from either WT or CCL5 KO mice prior to Ang II infusion. The experimental groups were designated as follows (n = 5 per group): WT + WT PL (WT mice reconstituted with WT platelets), WT + CCL5 KO PL (WT mice reconstituted with CCL5 KO platelets), and CCL5 KO + WT PL (CCL5 KO mice reconstituted with WT platelets). A Masson's trichrome staining of myocardial fibrosis (Scale bar: 100 μm). B Immunohistochemistry of α-SMA (Scale bar: 20 μm). C WGA staining showed cardiomyocyte cross-sectional area (Scale bar: 25 μm). D-E Immunohistochemical staining for platelets (CD41), CD8+ T cells, macrophages (MAC-2), and M2 macrophages (ARG-I) in heart tissue (Scale bar: 200 μm). Data are presented as mean ± standard deviation, with n representing the number of animals. * P < 0.001, *** P < 0.001, *** P < 0.001, NS indicating no significance.

To examine the direct impact of CCL5-activated platelets on M2 macrophage polarization, WT or CCL5 KO platelets were co-cultured with WT macrophages *in vitro*. In the presence of Ang II and ADP, macrophages co-cultured with CCL5 KO platelets exhibited a significant decrease in CD163 protein expression, as well as in the mRNA levels of *Arg1*, *Il10*, and *Mrc1*, compared to macrophages co-cultured with WT platelets (Figure 6E, F). To assess

the influence of M2 macrophages suppression by CCL5-deficient platelets on subsequent myofibroblast differentiation, fibroblasts were cultured with cell-free supernatants from macrophages co-cultured with either WT or CCL5 KO platelets. Fibroblasts exposed to supernatants from macrophages co-cultured with CCL5 KO platelets showed a marked reduction in α-SMA protein levels, along with decreased mRNA expression of *Col1a1*, *Col3a1*, *Sm22*, and *a-Sma*,

compared to those stimulated with supernatants from macrophages co-cultured with WT platelets (Figure 6G, То address potential H). the macrophage-intrinsic CCL5 deficiency to confound observed polarization effects. bone marrow-derived macrophages (BMDM) from WT and CCL5 KO mice were stimulated with Ang II in vitro. Gene expression analysis revealed no significant differences between the two groups in the expression of M1 macrophage markers (Mcp1, Tnfa, Il6, Inos, Cd80, and Cd86) or M2 macrophage markers (Tgfb1, Il10, Arg1, Mrc1, and Ym1) in response to Ang II stimulation (Figure S13A, B). Furthermore, supernatants collected from these stimulated macrophages exhibited comparable effects on myofibroblast differentiation (Figure S13C, D). This indicates that CCL5 deficiency within macrophages does not directly influence myofibroblast activation in results context. These suggest CCL5-mediated platelet activation plays a pivotal role in driving M2 macrophage polarization, which in turn promotes subsequent myofibroblast differentiation.

CCL5 deficiency reduces platelet-derived TGF- β 1 in cardiac remodeling

Platelets contain approximately 40 times more TGF-β1 than other cell types, which is released rapidly upon platelet activation [32]. Compared to BMDMs. splenocytes, cardiac fibroblast. cardiomyocytes and endothelial cells, only platelets rapidly released substantial amounts of TGF-β1 as soon as 10 minutes following ADP plus Ang II stimulation, with this effect persisting for up to 24 hours (Figure S14A). Upon 3 days of Ang II treatment, platelets were identified as the major contributor to cardiac TGF-β1 during the initial phase (Figure S14B). These demonstrate the crucial role of platelet-derived TGF-β1 in triggering Ang II-related pathological responses. This study investigated whether CCL5 deficiency could alleviate Ang II-promoted cardiac remodeling by suppressing platelet-derived TGF-β1. Following Ang II infusion, transcriptional upregulation of key components within the TGF-β pathway was observed in WT mice, an effect that was significantly attenuated in animals lacking CCL5 (Figure 7A). The gene expression of cardiac Ccl5 showed a strong positive correlation with Tgfb1 in Ang II-infused mice (Figure 7B). Additionally, the hearts of CCL5 KO mice exhibited a significant attenuation in the Ang II-induced elevation of TGF-β1 protein levels relative to WT controls (Figure 7C). Immunofluorescence analysis further verified that following Ang II stimulation, cardiac TGF-β1 expression and platelet infiltration (CD41-positive) were decreased in CCL5 KO mice, and TGF-β1 was

mainly found to co-localize with platelets (Figure 7D). In the platelet depletion/reconstitution model, WT mice that received CCL5 KO platelet transplants demonstrated markedly lower cardiac TGF-\(\beta\)1, both in protein content and mRNA expression, relative to those receiving WT platelets (Figure 7E, F). CCL5 KO platelets released less TGF-\$1 in the supernatant following ADP stimulation, compared to WT platelets (Figure 7G). Interestingly, more TGF-β1 was retained within CCL5 KO platelets after ADP stimulation (Figure 7H). Furthermore, recombinant TGF-β1 reversed the suppression of M2 markers in macrophages treated with supernatants from CCL5 KO platelets, as evidenced by upregulated mRNA expression of Arg1, Il10, Mrc1, and Ym1, along with increased protein levels of MRC-1 (Figure 7I, J). These results suggest that platelets are a major source of TGF-β1 in hypertensive cardiac remodeling and that CCL5 is essential for elevating platelet-derived TGF- β 1 to promote M2 polarization.

CCL5 deficiency dampens NF-кВ signaling activation in the heart and platelet

NF-κB signaling plays a critical role in cardiac inflammation and remodeling and is also known for involvement in platelet-mediated immune inflammation [33, 34]. To explore whether CCL5 promotes cardiac remodeling and platelet activation through NF-κB pathway enhancement, expression analysis was conducted. NF-kB signaling pathway genes showed upregulation in Ang II-treated WT hearts, which was notably reduced in CCL5 KO hearts (Figure 8A). Ang II promoted NF-кВ activation reflected by increased phosphorylation of P65 in WT hearts, which was significantly lowered by CCL5 KO (Figure 8B). The direct effect of CCL5 on NF-kB signaling in platelets was also assessed. CCL5 KO markedly reduced ADP-stimulated phosphorylation of P65 (Figure 8C). Inhibition of NF-kB signaling with BAY 11-7082 efficiently abrogated the enhancing effects of rmCCL5 on platelet P-selectin release and on platelet spreading (Figure 8D, E). Furthermore, rmCCL5 stimulation led to increased TGF-β1 secretion in WT platelets, an effect abolished by NF-κB inhibition (Figure 8F). Within platelets, TGF- β 1 is stored in α -granules, the secretion of which is linked to the actin cytoskeleton [35]. To determine whether CCL5 promotes α -granule release and TGF-β1 secretion by triggering rapid actin cytoskeleton remodeling via the NF-кb signaling, the morphology and distribution of F-actin in platelets after 10 min of rmCCL5 stimulation was detected. Immunofluorescence revealed polymerization increased upon rmCCL5 stimulation and reduced by NF-kB inhibitor (Figure S15).

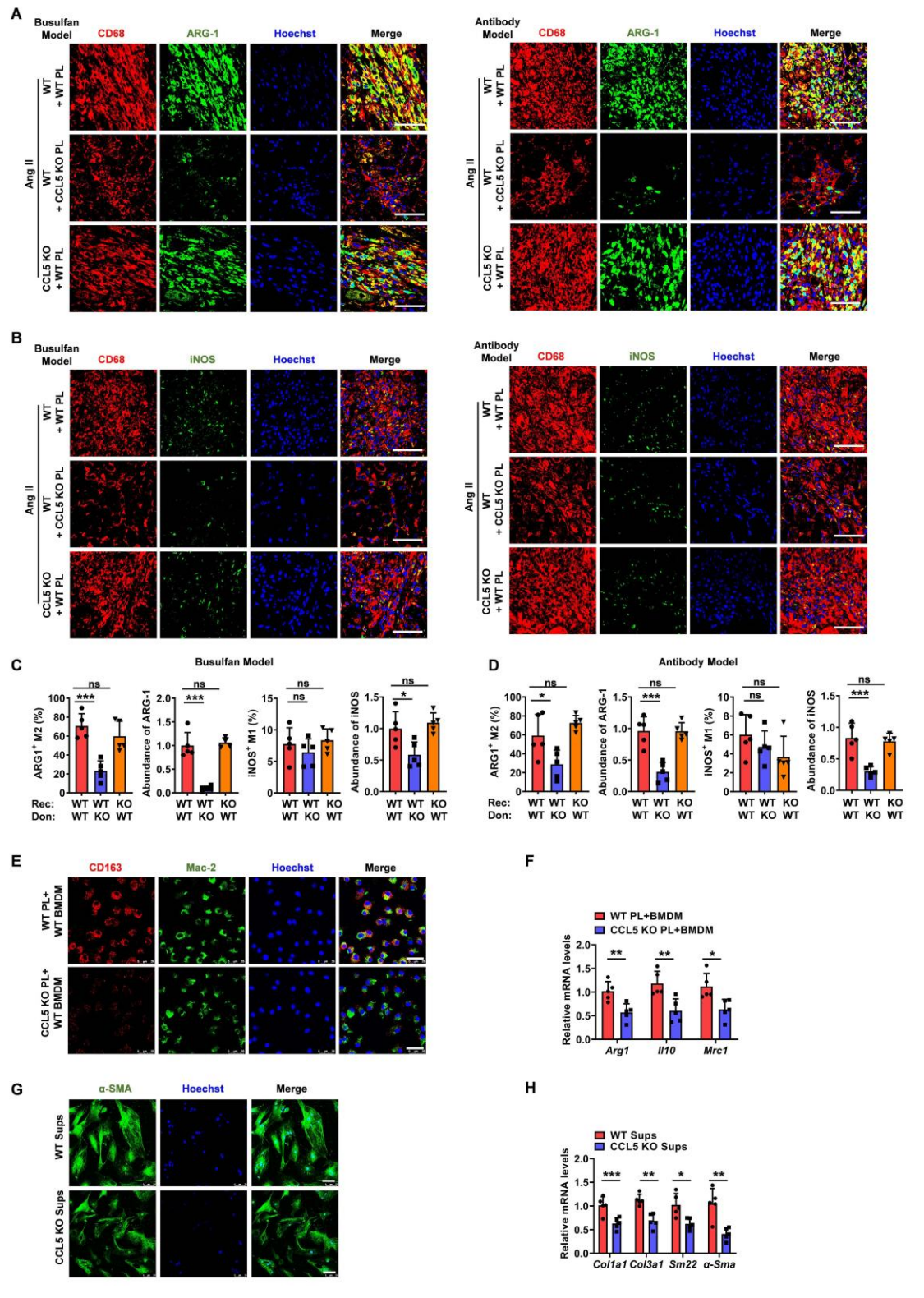


Figure 6. CCL5-deficient platelets attenuate Ang II-induced M2 macrophage polarization. Recipient mice underwent platelet depletion via either busulfan-induced chemotherapy or administration of the anti-platelet antibody. Subsequently, these mice were reconstituted with platelets derived from either WT or CCL5 KO mice before initiating Ang II infusion. The experimental groups were designated as follows (n = 5 per group): WT + WT PL (WT mice reconstituted with WT platelets), WT + CCL5 KO PL (WT mice reconstituted with CCL5 KO platelets), and CCL5 KO + WT PL (CCL5 KO mice reconstituted with WT platelets). Immunofluorescence of CD68 (red), ARG-I (green) (A) and iNOS (green) (B) in the heart (Scale bar: 50 μm). C, D The abundance and proportion of ARG-I+ M2 and iNOS+ MI macrophage were quantified. Bone marrow-derived macrophages (BMDM) were co-cultured with ADP-activated WT or CCL5 KO platelets in the presence of Ang II (100 nM) for 48 hours. Macrophages were analyzed for M2 markers, and the supernatants were collected for myofibroblasts minulation. E Immunofluorescence of CD I63 on macrophages (MAC-2) (n = 3; Scale bar: 25 μm). F Gene expression of M2 markers (Arg I., III 0, and Mrc I) in macrophages (n = 5). G Immunofluorescence of myofibroblasts with α-SMA (n = 3; Scale bar: 75 μm). H Gene expression of myofibroblast markers (Col I a I., Col3 a I., Sm22, and α-Sma) detected by RT-PCR (n = 5). Data are presented as mean ± standard deviation, with n representing the number of animals. * P < 0.05, ** P < 0.01, *** P < 0.001, NS indicating no significance.

These suggest that the NF- κ B pathway may regulate α -granules release and TGF- β 1 secretion by modulating the actin cytoskeleton. Macrophages treated with WT platelet supernatant in the presence of the NF- κ B inhibitor BAY 11-7082 exhibited downregulated expression of the M2 marker genes Mrc1 and Ym1 along with reduced MRC-1 protein levels, whereas the expression of Arg1 and Il10 remained unaffected (Figure S16).

While the expression of CCL5 receptors CCR1 and CCR3 on platelets has been confirmed, their specific biological functions in this context remain underexplored [15]. To elucidate the functional receptors responsible for CCL5-mediated effects on platelets, we utilized blocking antibodies targeting CCR1 and CCR3. Individual or combined application these antibodies effectively inhibited rmCCL5-stimulated platelet p65 phosphorylation, α-granule secretion, and TGF-β1 secretion (Figure 8G-I). Notably, no statistically significant difference in inhibitory efficacy was observed between the individual and combined antibody treatments (Figure 8G-I). These results suggest that CCL5 promotes platelet activation and TGF-β1 secretion via the NF-κB pathway, mediated by both CCR1 and CCR3. This mechanism further contributes to hypertensive cardiac remodeling.

Biological pathway networks modulated by CCL5 during hypertensive cardiac remodeling

To delineate the principal biological pathways contributes through which CCL5 hypertension-induced cardiac remodeling, performed a ClueGO-based functional annotation of CCL5-regulated genes. This analysis identified significant enrichment in multiple key processes, including immune activation, macrophage and T cell stimulation, platelet function, NIK/NF-kB signal transduction, TGF-β receptor signaling, extracellular matrix (ECM) assembly (Figure 9). Among these, molecules implicated in two or more functional clusters were Ccl5, Tgfb1, Tgfb2, Ltbp3, Emilin1, Fn1, Col1a2, Lox, Cd200, Itgb3, Trem2, Apoe, Ctss, Il6, Loxl3, Cx3cr1, Mdk, Cd44, Adam8, Nlrc3, and Laptm5 (Figure 9). Collectively, these results demonstrate that CCL5 promotes ECM deposition by orchestrating inflammatory responses involving platelets, macrophages, and T cells, primarily through activation of NF-κB and TGF-β signaling pathways in the hypertensive heart.

Discussion

Hypertensive cardiac remodeling markedly increases the risk of cardiovascular complications and is associated with adverse clinical outcomes.

However, current treatments for hypertensive cardiac remodeling are limited and often associated with considerable side effects [36]. Inflammation is a key driver in the onset of hypertension-induced damage to end organs. Our findings reveal an essential function of CCL5 in cardiac remodeling triggered by Ang II. CCL5 promotes platelet activation, facilitating cardiac inflammatory cascades and M2 macrophage polarization. Mechanistically, CCL5 activates NF-κB signaling via CCR1 and CCR3, leading to the upregulation of platelet-derived TGF-β1, which drives both M2 macrophage polarization and differentiation. myofibroblast Our results demonstrate that CCL5-mediated platelet activation contributes causally to the development of cardiac remodeling, thereby supporting the therapeutic potential of CCL5 inhibition in mitigating inflammatory processes associated with hypertensive heart remodeling.

CCL5 is elevated in various cardiovascular events, including hypertension, where it triggers the pathogenesis of cardiovascular dysfunction and renal [17, 37]. During pulmonary hypertension, CCL5 expression was associated with CD45+ inflammatory cell infiltration into the pulmonary artery wall, and CCL5 deletion attenuated Sugen5416/hypoxia-induced pulmonary hypertension and pulmonary vascular remodeling [38, 39]. Similarly, both pharmacological inhibition and genetic deletion of CCL5 mitigated Ang II-promoted vascular dysfunction in hypertension models [17]. In contrast, genetic deletion of CCL5 exacerbated kidney damage during Ang II-dependent hypertension [18]. According to previous research, in smooth muscle cells (VSMCs) spontaneously hypertensive rats (SHRs), CCL5 expression is suppressed by Ang II through 12-lipoxygenase (12-LO)-dependent mechanisms [40]. To elucidate the molecular mechanisms underlying early inflammatory response in cardiac remodeling, we established a mouse model of Ang II-induced cardiac hypertrophy via 7-day Ang II infusion. This model exhibits a compensatory elevation in cardiac function accompanied by pathological features such as myocardial fibrosis, hypertrophic remodeling, and inflammatory infiltration [4, 19, 41, 42]. Our study demonstrated that Ang II increased cardiac CCL5 expression and targeting CCL5 ameliorated Ang II-induced pathological cardiac remodeling, thereby ameliorating the early compensatory cardiac function elevation. In contrast to the chronic hypertension and vascular remodeling in SHRs, our model of Ang II-infused mice primarily induces acute cardiac injury and remodeling. The discrepancy in the regulation of

CCL5 by Ang II may be attributed to differences in the disease models and/or the distinct cell types involved. These disparate findings suggest that CCL5

plays context-dependent roles in hypertension-induced end-organ injury, a topic that remains under active investigation.

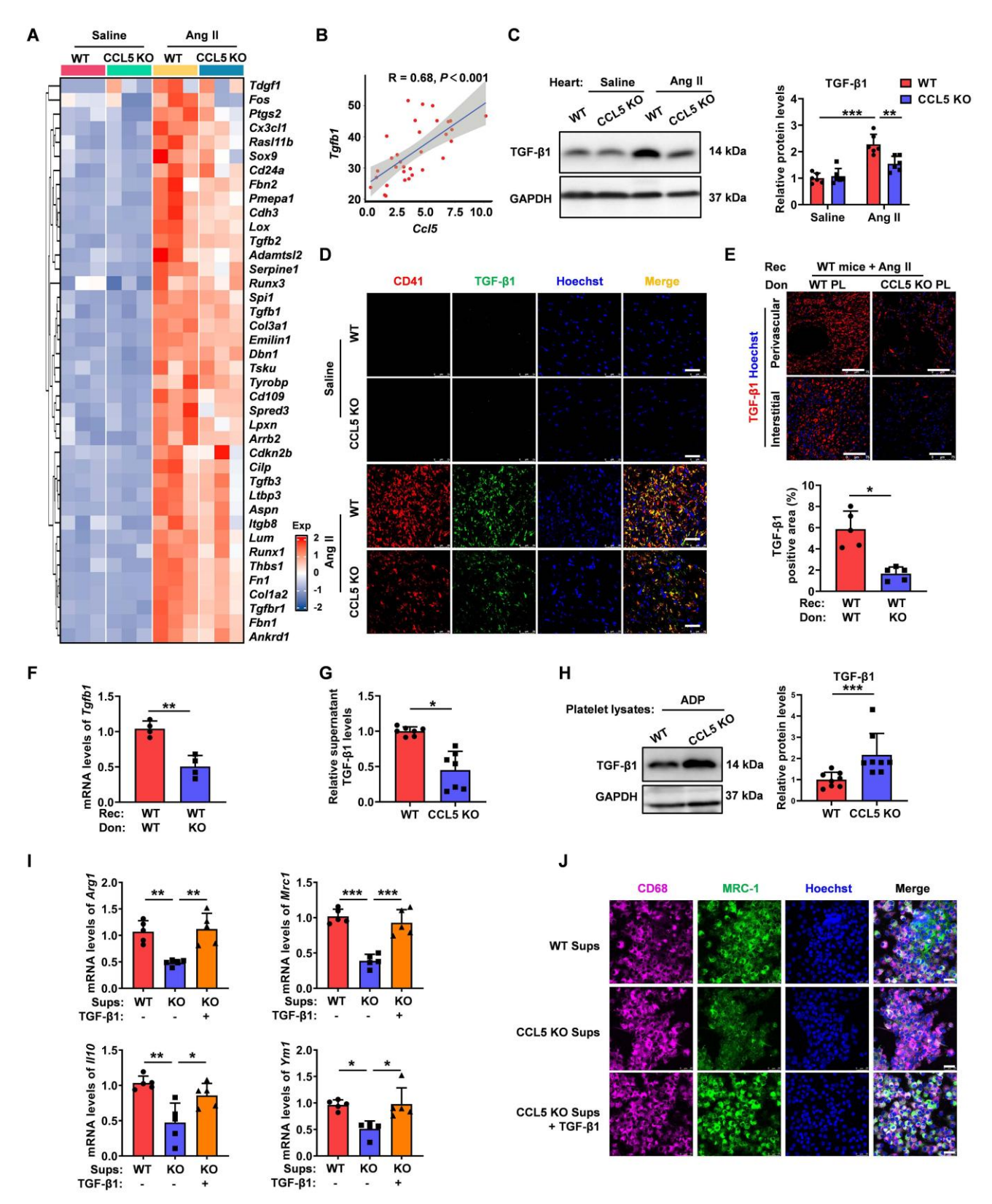


Figure 7. CCL5 deficiency reduces platelet-derived TGF- β 1 in cardiac remodeling. WT and CCL5 KO mice were subjected to a 7-day infusion of saline or Ang II. A Gene expression of the TGF- β signaling pathway in the hearts, detected by RNA sequencing (n = 3). **B** Correlation between *Cd5* and *Tgfb1* gene expression in hearts following a 7-day infusion of either Ang II or vehicle, using GEO datasets (n = 32). **C** TGF- β 1 protein levels in the heart analyzed by Western blotting (n = 6). **D** Immunofluorescence of

platelets (CD41, red) and TGF- β 1 (green) in the heart (n = 5; Scale bar: 25 μ m). WT mice were platelet depleted by busulfan, followed by reconstitution with platelets derived from either WT or CCL5 KO mice prior to Ang II infusion. **E** Immunofluorescence of TGF- β 1 (red) in the heart (n = 5; Scale bar: 75 μ m). **F** mRNA levels of Tgfb1 in the hearts detected by RT-PCR (n = 4). Washed platelets from WT and CCL5 KO mice were stimulated with ADP (10 μ M) for 10 minutes. TGF- β 1 levels were detected in the supernatants by ELISA (**G**) (n = 7) and in platelet lysates by Western blotting (**H**) (n = 8). Bone marrow-derived macrophages (BMDM) were co-cultured with supernatants from ADP plus Ang Il-activated WT or CCL5 KO platelets with or without TGF- β 1 (20 ng/mL) for 48 hours. Macrophages were analyzed for M2 markers. I Gene expression of M2 markers (Arg I, III0, MrcI and YmI) in macrophages (n = 5). J Immunofluorescence of MRC-I on macrophages (CD68) (n = 5; Scale bar: 25 μ m). Data are presented as mean \pm standard deviation, with n representing the number of animals. * P < 0.05, ** P < 0.01, *** P < 0.001.

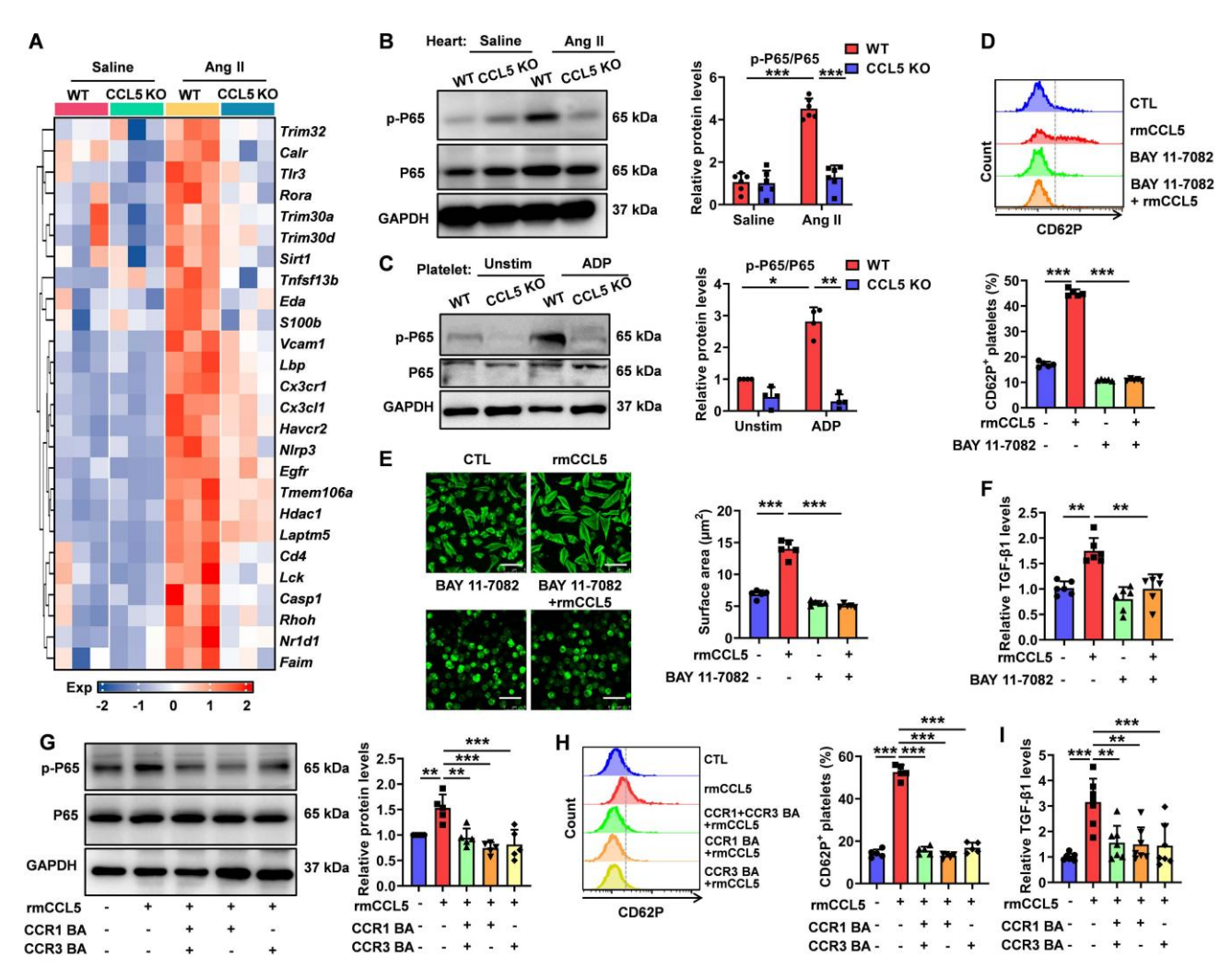


Figure 8. CCL5 deficiency dampens NF-κB signaling activation in the heart and platelets. WT and CCL5 KO mice were infused with saline or Ang II for 7 days. A Heatmap of NF-κB signaling pathway gene expression in hearts, analyzed by RNA sequencing (n = 3). B NF-κB activation in the heart, reflected by the p-P65/P65 protein ratio, was detected by Western blotting analysis (n = 6). C Washed platelets from WT and CCL5 KO mice were stimulated with or without ADP (10 μM) for 10 minutes, and NF-κB activation was assessed by Western blotting (n = 4). WT platelets were pretreated with or without the NF-κB inhibitor BAY 11-7082 (1 μM) for 15 minutes, followed by stimulation with rmCCL5 (100 ng/mL) in the presence of ADP (5 μM) for 10 minutes in vitro. D The percentage of CD62P-positive platelets after rmCCL5 stimulated for 10 minutes was measured by flow cytometry (n = 5). E Representative images of platelets spreading on fibrinogen-coated wells at 37°C for 2 hours and quantification of spread area (μm²) (n = 5; Scale bar: 8 μm). F TGF-β1 levels in supernatants of platelets detected by ELISA (n = 6). WT platelets were pretreated with CCR1 and CCR3 blocking antibodies (CCR1 BA and CCR3 BA) alone or in combination for 15 minutes, followed by stimulation with rmCCL5 (100 ng/mL) in the presence of ADP (5 μM) for 5 minutes in vitro. G Western blotting analysis of NF-κB activation (n = 5). H The percentage of CD62P-positive platelets was measured by flow cytometry (n = 5). I TGF-β1 levels in supernatants were detected by ELISA (n = 7). Data are presented as mean ± standard deviation, with n representing the number of animals. * P < 0.05, *** P < 0.01, ***** P < 0.001.

Previous studies have established that CCL5 modulates inflammatory diseases primarily by influencing the biology of T lymphocytes, monocytes, macrophages, and neutrophils [5, 16]. Increasing evidence highlights the inflammatory role of platelets in cardiovascular disease [43]. The protective effect of platelet inhibition has been observed in TAC-induced cardiac inflammation and fibrosis [7]. Platelets express CCL5 receptors, CCR1 and CCR3, and secrete

substantial amounts of CCL5 upon activation [15]. One study demonstrated that CCL5 induces rapid, dose-dependent Ca²⁺ responses in platelets and promotes platelet aggregation *via* a feedback mechanism involving ADP release and its subsequent binding to ADP receptors [15]. In contrast, another study reported no effect of CCL5 on Ca²⁺ flux in washed platelets or platelet aggregation in either washed platelets or platelets in platelet-rich plasma

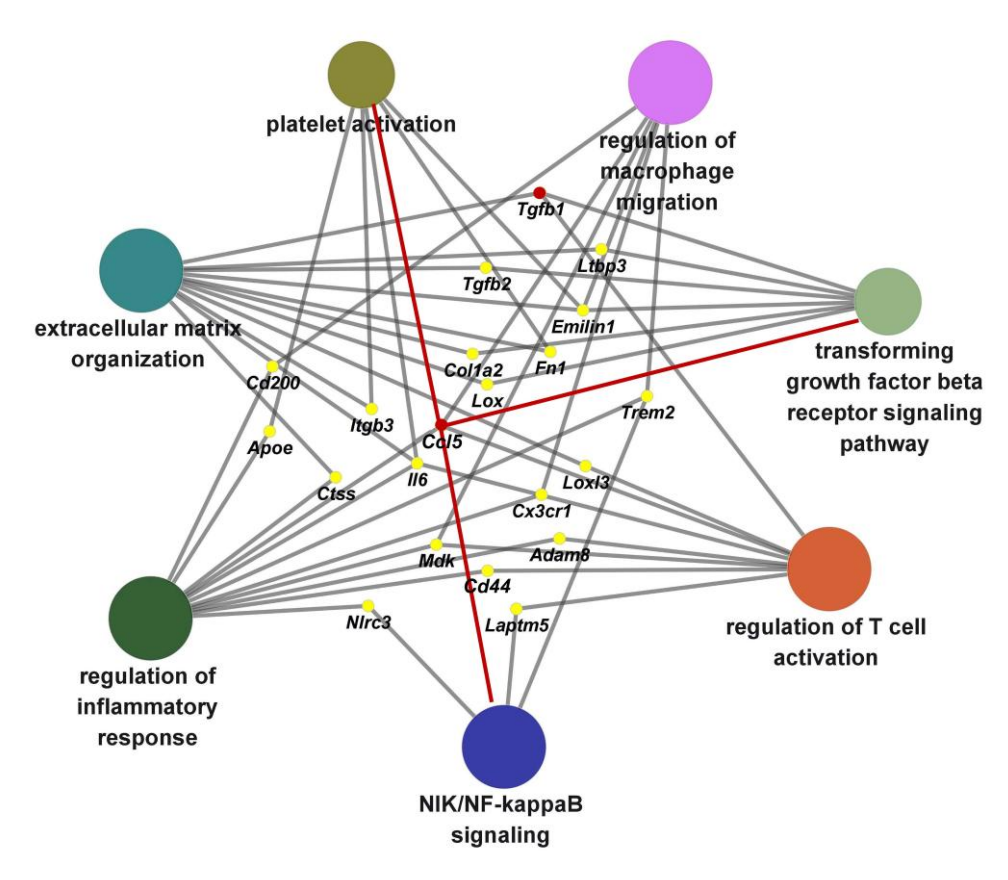


Figure 9. Biological pathway networks modulated by CCL5 during hypertensive cardiac remodeling. Functional enrichment analysis using ClueGO was performed on CCL5-dependent genes from Ang II-infused hearts, revealing functionally clustered Gene Ontology (GO) biological processes categorized by color. Key enriched terms included inflammatory response regulation, macrophage and T cell activation, platelet function, NIK/NF- κ B and TGF- β receptor signaling, and extracellular matrix organization. Nodes correspond to significantly enriched GO terms, with edges indicating shared genes between processes. Gray edges reflect connections established automatically by ClueGO, while red edges highlight novel interactions identified in this study.

(PRP) [14]. Thus, the direct effects of CCL5 on platelet function remain controversial. While previous studies have mainly focused on platelet aggregation regulation by CCL5, the role of CCL5 in platelet inflammation and its pathological significance remain poorly understood. In the present study, CCL5 was identified as a master regulator of platelet inflammatory activation. Our findings show that CCL5 directly modulates platelet α -granule release and TGF- β 1 secretion. Pharmacological platelet inhibition and platelet depletion/reconstitution experiments provide further evidence for the critical role of CCL5-mediated platelet function in promoting cardiac inflammation and remodeling during Ang II-induced hypertension.

Through direct cellular contacts as well as secretory factors such as cytokines and microvesicles, platelets are pivotal in mediating leukocyte recruitment and activation, thereby fundamentally contributing to the onset and advancement of inflammatory disorders [6]. Consequently, the diminished immune cell infiltration within the cardiac tissue of CCL5 KO mice following Ang II infusion can be attributed to both a blunted platelet-mediated

inflammatory response and a reduction in direct chemotaxis resulting from CCL5 deficiency. Given the established roles of CD8+ T cells and macrophages in the pathogenesis and progression of cardiac remodeling [44, 45], the observed decrease in these cell populations, stemming from impaired platelet activation, likely further contributed to the attenuation of cardiac inflammation. Platelets regulate macrophage function by modulating activation, polarization, and differentiation. One demonstrated that platelets promote pro-inflammatory iNOS+ macrophage polarization and bacterial clearance, thereby increasing survival in septic mice Additionally, platelets enhance NLRP3 inflammasome activation and boost IL-1β secretion in macrophages [47]. Conversely, platelet-derived THBS1 promotes the cycling of M2 macrophages, which exhibit a pro-repair M2 phenotype and enhanced proliferative activity during renal injury repair [48]. In bacterial-induced pneumonia, platelets are recruited to the lung alongside neutrophils and regulatory Τ cells, modulating macrophage polarization toward an anti-inflammatory phenotype during the resolution phase [49]. These studies

suggest that the role of platelets in macrophage polarization varies depending on the specific inflammatory disease context. Our present work demonstrated a pivotal role for CCL5-dependent platelet activation in promoting M2 polarization to facilitate cardiac remodeling during Ang II infusion. This was further confirmed by *in vitro* co-culture experiments showing the direct effects of CCL5/platelet interaction on M2 polarization in the presence of Ang II.

Previous study showed that platelet-derived TGF-β1 contributes to plasma levels of TGF-β1 and the pathological cardiac changes occurring in response to aortic constriction [8]. Our study revealed platelet-derived TGF-\u00ed1 was the major source of TGF-β1 in Ang II-induced early cardiac remodeling. Platelet-derived TGF-β1 needs to be activated to interact with its receptors, and Ang II infusion created conditions with multiple latent TGF-\beta1 activators, including thrombospondin-1, matrix metalloproteinases, RGD (Arg-Gly-Asp)-binding integrins, and reactive oxygen species [50-53]. Platelets can quickly release large amounts of TGF-β1. In contrast, in other cardiac cells, Ang II mainly regulated TGF-\beta1 expression through transcriptional control or by triggering phenotypic changes, which process was relatively slow and happened as a delayed response after platelet activation. Thus, platelets appear to be a key player in the pathological cardiac remodeling triggered by Ang II, potentially cascade of pro-inflammatory multi-cellular events. CCL5 KO reduced platelet activation, which may weaken the platelet-driven initiation and amplification of inflammatory responses These included decreased infiltration of macrophages and CD8+ T cells, reduced M2 macrophage polarization, less fibroblast proliferation, and diminished myocardial hypertrophy, thereby lowering TGF-β1 levels from these cells. Overall, suppression of platelet activation is pivotal to ameliorating cardiac remodeling in CCL5 KO mice through the general reduction of inflammation in the cardiac environment.

NF-κB signaling plays a key role in hypertensive cardiac remodeling and inflammation [33]. Numerous studies have confirmed its involvement in platelet-mediated immune inflammation [34]. However, the specific NF-κB signaling pathway in platelets is not fully understood. Our data demonstrated a positive correlation between *Ccl5* expression and NF-κB signaling gene expression. CCL5 KO downregulated NF-κB signaling activation in Ang II-infused hearts and ADP-stimulated platelets. Furthermore, inhibition of NF-κB signaling abolished rmCCL5-induced platelet α-granule release

and TGF- $\beta1$ secretion. Within platelets, TGF- $\beta1$ is stored in α -granules, the secretion of which is linked to the actin cytoskeleton [35]. Blocking NF- κ B signaling impeded CCL5-induced rapid F-actin polymerization. This suggests that the NF- κ B pathway may regulate TGF- $\beta1$ release from α -granules by modulating the actin cytoskeleton, although the precise molecular mechanisms require further elucidation. Furthermore, this study provides novel evidence of the biological functions of CCR1 and CCR3 receptors on platelets, indicating that CCL5 modulates NF- κ B signaling through these receptors to promote platelet activation.

This study presents several limitations and suggests potential future directions. The findings from global CCL5 KO mice do not rule out the possible involvement of CCL5 produced by cells other than platelets in Ang II-promoted cardiac remodeling, including T cells, macrophages, endothelial cells, fibroblasts, smooth muscle cells, and cardiomyocytes. CCL5 released by these cells might contribute to disease development by modulating immune cell infiltration, angiogenesis, and VSMCs proliferation [5, 16, 54, 55]. Although our platelet transfusion experiments have demonstrated the essential and unique role of platelet-derived CCL5, further research using cell-specific knockout mouse models is needed to clarify the distinct roles of CCL5 from various cell sources. CCL5 exerts its biological effects through various receptors, including CCR1, CCR3, and CCR5. However, these receptors can also be engaged by alternative ligands; thus, strategies that inhibit a single receptor may offer only a partial view of CCL5's broad spectrum of activities and cannot preclude compensatory effects from other chemokine signaling pathways. For instance, prior research has shown that CCR5 deficiency did not attenuate injury to the heart and kidneys following treatment with DOCA-salt in combination with Ang II [56]. While our study showed that CCL5-deficient mice are protected from Ang II-promoted cardiac remodeling, this discrepancy may be attributed to differences in mouse strains and the severity of the hypertension model. Further investigation of CCL5 receptors in the context of Ang II-induced cardiac remodeling would be valuable and is an area for future research. While our analysis of blood pressure in mice utilized the tail-cuff method, and revealed no substantial differences in average systolic blood pressure between CCL5 KO and WT mice in response to Ang II, consistent with prior studies employing radiotelemetry [17, 18], we acknowledge the inherent limitations of this technique. The tail-cuff method, while providing an average blood pressure reading over several minutes, lacks the capacity to capture dynamic hemodynamic

fluctuations occurring throughout the day or during unrestricted activity [57]. To mitigate potential inaccuracies and ensure comparability between groups, we adhered to a standardized procedure for tail-cuff measurements, focusing on average blood pressure rather than transient variations. In contrast, implantable radiotelemetry offers continuous and blood pressure monitoring, assessment of temporal changes, including diurnal variations in hemodynamics, in freely moving animals. However, radiotelemetry is an invasive procedure associated with significant mortality and its cost restricts widespread morbidity, and implementation. Furthermore, the extensive instrumentation involved may influence inflammation; therefore, assessment of immune cell infiltration into target organs, circulating cytokines, chemokine levels in separate, non-instrumented animals is often preferred [58]. The primary objective of this study was to investigate the immune mechanisms underlying CCL5-mediated hypertensive cardiac remodeling, and blood pressure effects were not the focus of this immune-centric mechanism. Considering constraints in experimental conditions and the availability of transgenic mice, we employed the non-invasive tail-cuff method. Future investigations incorporating continuous radiotelemetry monitoring could offer more nuanced insights into the circadian profile and activity-related hemodynamic effects of CCL5 deletion hypertensive mice.

Conclusions

In summary, our findings identify CCL5 as a promising candidate for intervention in hypertensive cardiac remodeling. Inhibition of CCL5 signaling attenuates structural and functional abnormalities of the heart, including fibrosis, hypertrophy, and impaired function, triggered by Ang II. This research also represents the first exploration of CCL5's role in regulating platelet inflammatory activation and further investigates CCL5-dependent the platelet-primed inflammatory cascade, including promoting inflammatory cell recruitment and M2 macrophage polarization. Mechanistically, CCL5 promotes platelet-derived TGF-β1 secretion through the NF-κB signaling pathway via CCR1 and CCR3 receptors, thereby exerting pro-inflammatory and pro-fibrotic effects. Taken together, our results delineate the multiple functions of CCL5 in modulating platelet activation and macrophage polarization. These insights indicate that therapeutic intervention against this pathway and its associated platelet-macrophage crosstalk could represent a novel

approach to mitigate inflammatory responses and ameliorate cardiac remodeling.

Abbreviations

Ang II: angiotensin II; CCL5 KO: CCL5 knockout; WT: wild-type; rmCCL5: recombinant CCL5; TAC: transverse aortic constriction; CCL5: C-C chemokine motif ligand 5; NF-κB: factor-kappa B; TGF-β1: transforming growth factor-beta1; GSEA: gene set enrichment analysis; KEGG: kyoto encyclopedia of genes and genomes; GO: gene ontology; GSVA: gene set variation analysis; ASA: aspirin; CPG: clopidogrel; PRP: platelet-rich plasma; EF: ejection fraction; FS: fractional shortening; ESAWT: end-systolic anterior wall thickness; ESPWT: end-systolic posterior wall thickness; PCA: principal component analysis; DEGs: differentially expressed genes; THR: thrombin.

Supplementary Material

Supplementary figures and table. https://www.thno.org/v16p0689s1.pdf

Acknowledgments

All authors would like to thank the research groups for the GEO data cohort which provided data for this collection and expresses gratitude for the funding. We thank all of the members of the Biological Analysis Center at Institute of Materia Medica of Chinese Academy of Medical Sciences for the experimental platform.

Funding

This work was supported by the CAMS Innovation Fund for Medical Sciences (CIFMS) Grant (No. 2021-I2M-1-028) and Natural Science Foundation of China (NSFC) Grant (No. 81973325).

Author contributions

M.Y. and S.L. conceived the study and designed the experiments. S.L., Z.Z., and M.Z. carried out the experimental work. S.L., M.Z., T.L., F.Z., W.Z., and Y.Z. were responsible for data acquisition, performed data analysis and interpretation, and conducted statistical analyses. T.L., Y.H., Z.Y., and L.Y. offered technical assistance and contributed to statistical guidance. M.Y. secured funding and provided overall supervision. All authors critically reviewed the manuscript and approved the final version.

Data availability

The data that support the findings of this study are available from the corresponding author upon reasonable request. All RNA-seq data are available through the NCBI's GEO and can be accessed through GEO SuperSeries accession number GSE285383.

Competing Interests

The authors have declared that no competing interest exists.

References

- Kong P, Christia P, Frangogiannis NG. The pathogenesis of cardiac fibrosis. Cell Mol Life Sci. 2014; 71: 549-74.
- Forrester SJ, Booz GW, Sigmund CD, Coffman TM, Kawai T, Rizzo V, et al. Angiotensin II signal transduction: an update on mechanisms of physiology and pathophysiology. Physiol Rev. 2018; 98: 1627-738.
- Yang M, Zheng J, Miao Y, Wang Y, Cui W, Guo J, et al. Serum-glucocorticoid regulated kinase 1 regulates alternatively activated macrophage polarization contributing to angiotensin II-induced inflammation and cardiac fibrosis. Arterioscler Thromb Vasc Biol. 2012; 32: 1675-86.
- Wang L, Zhang YL, Lin QY, Liu Y, Guan XM, Ma XL, et al. CXCL1-CXCR2 axis mediates angiotensin II-induced cardiac hypertrophy and remodelling through regulation of monocyte infiltration. Eur Heart J. 2018; 39: 1818-31.
- Mikolajczyk TP, Szczepaniak P, Vidler F, Maffia P, Graham GJ, Guzik TJ. Role of inflammatory chemokines in hypertension. Pharmacol Ther. 2021; 223: 107799.
- Scherlinger M, Richez C, Tsokos GC, Boilard E, Blanco P. The role of platelets in immune-mediated inflammatory diseases. Nat Rev Immunol. 2023; 23: 495-510.
- Wu L, Zhao F, Dai M, Li H, Chen C, Nie J, et al. P2y12 receptor promotes pressure overload-induced cardiac remodeling via platelet-driven inflammation in mice. Hypertension. 2017; 70: 759-69.
- Meyer A, Wang W, Qu J, Croft L, Degen JL, Coller BS, et al. Platelet TGF-β1 contributions to plasma TGF-β1, cardiac fibrosis, and systolic dysfunction in a mouse model of pressure overload. Blood. 2012; 119: 1064-74.
- Liu Y, Lv H, Tan R, An X, Niu XH, Liu YJ, et al. Platelets promote Ang II (Angiotensin II)-induced atrial fibrillation by releasing TGF-β1 (Transforming Growth Factor-β1) and interacting With Fibroblasts. Hypertension. 2020; 76: 1856-67
- Jia LX, Qi GM, Liu O, Li TT, Yang M, Cui W, et al. Inhibition of platelet activation by clopidogrel prevents hypertension-induced cardiac inflammation and fibrosis. Cardiovasc Drugs Ther. 2013; 27: 521-30.
- Frangogiannis NG. Cardiac fibrosis: Cell biological mechanisms, molecular pathways and therapeutic opportunities. Mol Aspects Med. 2019; 65: 70-99.
- Läubli H, Spanaus KS, Borsig L. Selectin-mediated activation of endothelial cells induces expression of CCL5 and promotes metastasis through recruitment of monocytes. Blood. 2009; 114: 4583-91.
- Swanson BJ, Murakami M, Mitchell TC, Kappler J, Marrack P. RANTES production by memory phenotype T cells is controlled by a posttranscriptional, TCR-dependent process. Immunity. 2002; 17: 605-15.
- Shenkman B, Brill A, Brill G, Lider O, Savion N, Varon D. Differential response of platelets to chemokines: RANTES non-competitively inhibits stimulatory effect of SDF-1 alpha. J Thromb Haemost. 2004; 2: 154-60.
- Clemetson KJ, Clemetson JM, Proudfoot AE, Power CA, Baggiolini M, Wells TN. Functional expression of CCR1, CCR3, CCR4, and CXCR4 chemokine receptors on human platelets. Blood. 2000; 96: 4046-54.
- Marques RE, Guabiraba R, Russo RC, Teixeira MM. Targeting CCL5 in inflammation. Expert Opin Ther Targets. 2013; 17: 1439-60.
- Mikolajczyk TP, Nosalski R, Szczepaniak P, Budzyn K, Osmenda G, Skiba D, et al. Role of chemokine RANTES in the regulation of perivascular inflammation, T-cell accumulation, and vascular dysfunction in hypertension. FASEB J. 2016; 30: 1987-99.
- Rudemiller NP, Patel MB, Zhang JD, Jeffs AD, Karlovich NS, Griffiths R, et al. C-C Motif Chemokine 5 attenuates angiotensin II-dependent kidney injury by limiting renal macrophage infiltration. Am J Pathol. 2016; 186: 2846-56.
- Lv SL, Zeng ZF, Gan WQ, Wang WQ, Li TG, Hou YF, et al. Lp-PLA2 inhibition prevents Ang II-induced cardiac inflammation and fibrosis by blocking macrophage NLRP3 inflammasome activation. Acta Pharmacol Sin. 2021; 42: 2016-32.
- Lauer A, Schlunk F, Van Cott EM, Steinmetz H, Lo EH, Foerch C. Antiplatelet pretreatment does not increase hematoma volume in experimental intracerebral hemorrhage. J Cereb Blood Flow Metab. 2011; 31: 1736-42.
- Sirois MG, Simons M, Kuter DJ, Rosenberg RD, Edelman ER. Rat arterial wall retains myointimal hyperplastic potential long after arterial injury. Circulation. 1997; 96: 1291-8.
- Becht E, Giraldo NA, Lacroix L, Buttard B, Elarouci N, Petitprez F, et al. Estimating the population abundance of tissue-infiltrating immune and stromal cell populations using gene expression. Genome Biol. 2016; 17: 218.
- Racle J, de Jonge K, Baumgaertner P, Speiser DE, Gfeller D. Simultaneous enumeration of cancer and immune cell types from bulk tumor gene expression data. Elife. 2017; 6: e26476.

- Li T, Fan J, Wang B, Traugh N, Chen Q, Liu JS, et al. TIMER: a web server for comprehensive analysis of tumor-infiltrating immune cells. Cancer Res. 2017; 77: e108-e10.
- Li T, Fu J, Zeng Z, Cohen D, Li J, Chen Q, et al. TIMER2.0 for analysis of tumor-infiltrating immune cells. Nucleic Acids Res. 2020; 48: W509-w14.
- Finotello F, Mayer C, Plattner C, Laschober G, Rieder D, Hackl H, et al. Molecular and pharmacological modulators of the tumor immune contexture revealed by deconvolution of RNA-seq data. Genome Med. 2019; 11: 34.
- Chen B, Khodadoust MS, Liu CL, Newman AM, Alizadeh AA. Profiling tumor infiltrating immune cells with CIBERSORT. Methods Mol Biol. 2018; 1711: 243-59.
- Zhou M, Li T, Lv S, Gan W, Zhang F, Che Y, et al. Identification of immune-related genes and small-molecule drugs in hypertension-induced left ventricular hypertrophy based on machine learning algorithms and molecular docking. Front Immunol. 2024; 15: 1351945.
- Chi G, Lu J, He T, Wang Y, Zhou X, Zhang Y, et al. High mobility group box-1
 protein promotes astrocytic CCL5 production through the MAPK/NF-κB
 pathway following spinal cord injury. Sci Rep. 2024; 14: 22344.
- Ir MRGRJN, Shah A, Rivera-Amill V, Kumar A. Human immunodeficiency virus type 1 viral protein R (Vpr) induces CCL5 expression in astrocytes via PI3K and MAPK signaling pathways. J Neuroinflammation. 2013; 10: 136.
- Picardo M, Johansen C, Rittig AH, Mose M, Bertelsen T, Weimar I, et al. STAT2 is involved in the pathogenesis of psoriasis by promoting CXCL11 and CCL5 production by keratinocytes. PLoS One. 2017; 12: e0176994.
- Ahamed J, Burg N, Yoshinaga K, Janczak CA, Rifkin DB, Coller BS. In vitro and in vivo evidence for shear-induced activation of latent transforming growth factor-beta1. Blood. 2008; 112: 3650-60.
- Kawano S, Kubota T, Monden Y, Kawamura N, Tsutsui H, Takeshita A, et al. Blockade of NF-kappaB ameliorates myocardial hypertrophy in response to chronic infusion of angiotensin II. Cardiovasc Res. 2005; 67: 689-98.
- Kojok K, El-Kadiry AE, Merhi Y. Role of NF-κB in platelet function. Int J Mol Sci. 2019: 20.
- Flaumenhaft R, Dilks JR, Rozenvayn N, Monahan-Earley RA, Feng D, Dvorak AM. The actin cytoskeleton differentially regulates platelet α-granule and dense-granule secretion. Blood. 2005; 105: 3879-87.
- Carey RM, Moran AE, Whelton PK. Treatment of hypertension: a review. JAMA. 2022; 328: 1849-61.
- Costa RM, Cerqueira DM, Bruder-Nascimento A, Alves JV, Awata WMC, Singh S, et al. Role of the CCL5 and its receptor, CCR5, in the genesis of aldosterone-induced hypertension, vascular dysfunction, and end-organ damage. Hypertension. 2024; 81: 776-86.
- Nie X, Tan J, Dai Y, Liu Y, Zou J, Sun J, et al. CCL5 deficiency rescues pulmonary vascular dysfunction, and reverses pulmonary hypertension via caveolin-1-dependent BMPR2 activation. J Mol Cell Cardiol. 2018; 116: 41-56.
- Dorfmüller P, Zarka V, Durand-Gasselin I, Monti G, Balabanian K, Garcia G, et al. Chemokine RANTES in severe pulmonary arterial hypertension. Am J Respir Crit Care Med. 2002; 165: 534-9.
- Yun YH, Kim HY, Do BS, Kim HS. Angiotensin II inhibits chemokine CCL5 expression in vascular smooth muscle cells from spontaneously hypertensive rats. Hypertens Res. 2011; 34: 1313-20.
- Revelo XS, Parthiban P, Chen C, Barrow F, Fredrickson G, Wang H, et al. Cardiac resident macrophages prevent fibrosis and stimulate angiogenesis. Circ Res. 2021; 129: 1086-101.
- 42. Wang M, Han X, Yu T, Wang M, Luo W, Zou C, et al. OTUD1 promotes pathological cardiac remodeling and heart failure by targeting STAT3 in cardiomyocytes. Theranostics. 2023; 13: 2263-80.
- Totani L, Evangelista V. Platelet-leukocyte interactions in cardiovascular disease and beyond. Arterioscler Thromb Vasc Biol. 2010; 30: 2357-61.
- Rurik JG, Aghajanian H, Epstein JA. Immune cells and immunotherapy for cardiac injury and repair. Circ Res. 2021; 128: 1766-79.
- Brassington K, Kanellakis P, Cao A, Toh B-H, Peter K, Bobik A, et al. Crosstalk between cytotoxic CD8+ T cells and stressed cardiomyocytes triggers development of interstitial cardiac fibrosis in hypertensive mouse hearts. Front Immunol. 2022; 13: 1040233.
- Carestia A, Mena HA, Olexen CM, Ortiz Wilczyński JM, Negrotto S, Errasti AE, et al. Platelets promote macrophage polarization toward pro-inflammatory phenotype and increase survival of septic mice. Cell Rep. 2019; 28: 896-908.e5.
- Rolfes V, Ribeiro LS, Hawwari I, Böttcher L, Rosero N, Maasewerd S, et al. Platelets fuel the inflammasome activation of innate immune cells. Cell Rep. 2020; 31: 107615.
- Liu J, Zheng B, Cui Q, Zhu Y, Chu L, Geng Z, et al. Single-cell spatial transcriptomics unveils platelet-fueled cycling macrophages for kidney fibrosis. Adv Sci (Weinh). 2024; 11: e2308505.
- Rossaint J, Thomas K, Mersmann S, Skupski J, Margraf A, Tekath T, et al. Platelets orchestrate the resolution of pulmonary inflammation in mice by T reg cell repositioning and macrophage education. J Exp Med. 2021; 218: e20201353.
- Song H, Ren J. Protocatechuic acid attenuates angiotensin II-induced cardiac fibrosis in cardiac fibroblasts through inhibiting the NOX4/ROS/p38 signaling pathway. Phytother Res. 2019; 33: 2440-7.
- Mu D, Cambier S, Fjellbirkeland L, Baron JL, Munger JS, Kawakatsu H, et al. The integrin alpha(v)beta8 mediates epithelial homeostasis through MT1-MMP-dependent activation of TGF-beta1. J Cell Biol. 2002; 157: 493-507.

- Belmadani S, Bernal J, Wei CC, Pallero MA, Dell'italia L, Murphy-Ullrich JE, et al. A thrombospondin-1 antagonist of transforming growth factor-beta activation blocks cardiomyopathy in rats with diabetes and elevated angiotensin II. Am J Pathol. 2007; 171: 777-89.
- Akasaka E, Kleiser S, Sengle G, Bruckner-Tuderman L, Nyström A. Diversity
 of mechanisms underlying latent TGF-β activation in recessive dystrophic
 epidermolysis bullosa. J Invest Dermatol. 2021; 141: 1450-60.e9.
- Kim JH, Kim HS. Downregulation of angiotensin II-induced 12-lipoxygenase expression and cell proliferation in vascular smooth muscle cells from spontaneously hypertensive rats by CCL5. Korean J Physiol Pharmacol. 2009; 13: 385-92.
- Caballero EP, Santamaría MH, Corral RS. Endogenous osteopontin induces myocardial CCL5 and MMP-2 activation that contributes to inflammation and cardiac remodeling in a mouse model of chronic Chagas heart disease. Biochim Biophys Acta Mol Basis Dis. 2018; 1864: 11-23.
- Krebs C, Fraune C, Schmidt-Haupt R, Turner JE, Panzer U, Quang MN, et al. CCR5 deficiency does not reduce hypertensive end-organ damage in mice. Am J Hypertens. 2012; 25: 479-86.
- Luther JM, Fogo AB. Under pressure how to assess blood pressure in rodents; tail-cuff? Kidney Int. 2019; 96: 34-6.
- Harrison DG, Bader M, Lerman LO, Fink G, Karumanchi SA, Reckelhoff JF, et al. Tail-cuff versus radiotelemetry to measure blood pressure in mice and rats. Hypertension. 2024; 81: 3-5.